# Ant Colony Optimizations for Resource- and Timing-Constrained Operation Scheduling

Gang Wang, *Member, IEEE*, Wenrui Gong, *Student Member, IEEE*, Brian DeRenzi, *Student Member, IEEE*, and Ryan Kastner, *Member, IEEE*

***Abstract*—Operation scheduling (OS) is a fundamental problem in mapping an application to a computational device. It takes a behavioral application specification and produces a schedule to minimize either the completion time or the computing resources required to meet a given deadline. The OS problem is $\mathcal{NP}$-hard; thus, effective heuristic methods are necessary to provide qualitative solutions. We present novel OS algorithms using the ant colony optimization approach for both timing-constrained scheduling (TCS) and resource-constrained scheduling (RCS) problems. The algorithms use a unique hybrid approach by combining the MAX–MIN ant system metaheuristic with traditional scheduling heuristics. We compiled a comprehensive testing benchmark set from real-world applications in order to verify the effectiveness and efficiency of our proposed algorithms. For TCS, our algorithm achieves better results compared with force-directed scheduling on almost all the testing cases with a maximum 19.5% reduction of the number of resources. For RCS, our algorithm outperforms a number of different list-scheduling heuristics with better stability and generates better results with up to 14.7% improvement. Our algorithms outperform the simulated annealing method for both scheduling problems in terms of quality, computing time, and stability.**

***Index Terms*—Force-directed scheduling (FDS), list scheduling, operation scheduling (OS), MAX–MIN ant system (MMAS).**

## I. Introduction

As THE fabrication technology advances and transistors become more plentiful, modern computing systems can achieve better system performance by increasing the amount of computation units. It is estimated that we will be able to integrate more than half a billion transistors on a 468-mm$^2$ chip by the year 2009 [1]. This yields tremendous potential for future computing systems; however, it imposes big challenges on how to effectively use and design such complicated systems.

As computing systems become more complex, so do the applications that can run on them. Designers will increasingly rely on automated design tools in order to map applications onto these systems. One fundamental process of these tools is mapping a behavioral application specification to the computing system. For example, the tool may take a C function and create the code to program a microprocessor. This is viewed as software compilation. Or the tool may take a transaction level behavior and create a register transfer level circuit description. This is called hardware or behavioral synthesis. Both software and hardware synthesis flows are essential for the use and design of future computing systems.

Operation scheduling (OS) is an important problem in software compilation and hardware synthesis. An inappropriate scheduling of the operations can fail to exploit the full potential of the system. OS appears in a number of different problems, e.g., compiler design for superscalar and very long instruction word microprocessors [2], distributed clustering computation architectures [3], and behavioral synthesis of application-specified integrated circuit (ASICs) and field-programmable gate arrays (FPGAs) [4]. In this paper, we focus on OS for behavioral synthesis for ASICs/FPGAs. However, the basic algorithms proposed here can be modified to handle a wide variety of OS problems.

OS is performed on a behavioral description of the application. This description is typically decomposed into several blocks (e.g., basic blocks), and each of the blocks is represented by a data flow graph (DFG). Fig. 1 shows an example DFG for a 1-D eight-point fast discrete cosine transformation (DCT).

OS can be classified as resource-constrained scheduling (RCS) or timing-constrained scheduling (TCS). Given a DFG, clock cycle time, resource count, and resource delays, an RCS finds the minimum number of clock cycles needed to execute the DFG. On the other hand, TCS tries to determine the minimum number of resources needed for a given deadline.

In the TCS problem (also called fixed control step scheduling), the target is to find the minimum computing resource cost under a set of given types of computing units and a predefined latency deadline. For example, in many digital signal processing (DSP) systems, the sampling rate of the input data stream dictates the maximum time allowed for computation on the present data sample before the next sample arrives. Since the sampling rate is fixed, the main objective is to minimize the cost of the hardware. Given the clock cycle time, the sampling rate can be expressed in terms of the numbers of cycles that are required to execute the algorithm.

RCS is also found frequently in practice. This is because in many cases, the number of resources is known *a priori*. For instance, in software compilation for microprocessors, the computing resources are fixed. In hardware compilation, DFGs are often constructed and scheduled almost independently. Furthermore, if we want to maximize resource sharing, each block should use same or similar resources, which is hardly ensured by time-constrained schedulers. The time constraint of each

Manuscript received December 7, 2005; revised June 6, 2006. This work was supported in part by the National Science Foundation under Grant CNS-0524771. This paper was recommended by Associate Editor R. Camposano.

G. Wang and R. Kastner are with the Department of Electrical and Computer Engineering, University of California, Santa Barbara, CA 93106-9560 USA.

W. Gong is with Mentor Graphics Corporation, Wilsonville, OR 97070-7777 USA.

B. DeRenzi is with the Department of Computer Science and Engineering, University of Washington, Seattle, WA 98195-2350 USA.

Digital Object Identifier 10.1109/TCAD.2006.885829

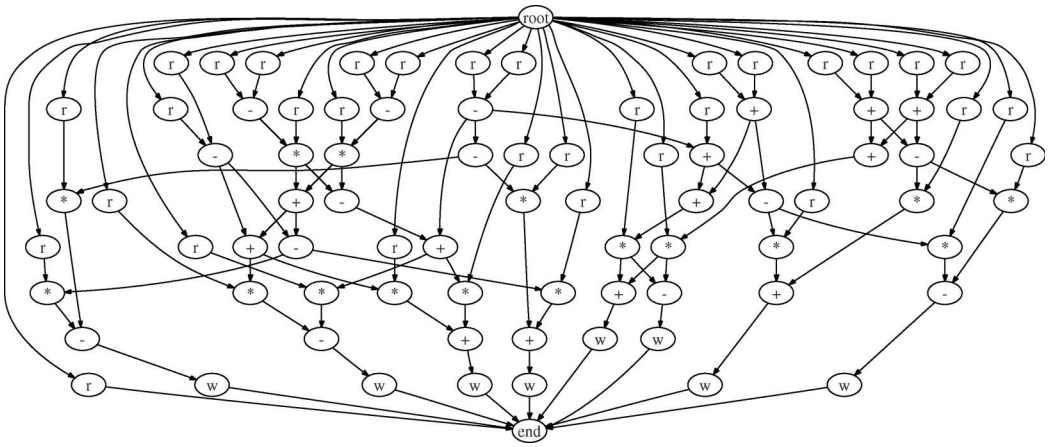


Fig. 1. DFG of the COSINE2 benchmark ("r" is for memory read and "w" for memory write).

block is not easy to define since blocks are typically serialized and budgeting global performance constraint for each block is not trivial.

OS methods can be further classified as static scheduling and dynamic scheduling [5]. Static OS is performed during the compilation of the application. Once an acceptable scheduling solution is found, it is deployed as part of the application image. In dynamic scheduling, a dedicated system component makes scheduling decisions on-the-fly. Dynamic scheduling methods must minimize the program's completion time while considering the overhead paid for running the scheduler.

In this paper, we focus on both resource- and timing-constrained static OS. We propose iterative algorithms based on the MAX–MIN ant colony optimization (ACO) for solving these problems. In our algorithms, a collection of agents (ants) cooperate together to search for a solution. Global and local heuristics are combined in a stochastic decision-making process in order to efficiently explore the search space. The quality of the resultant schedules is evaluated and fed back to dynamically adjust the heuristics for future iterations. The main contribution of this paper is the formulation of scheduling algorithms that:

1) utilize a unique hybrid approach combining traditional heuristics and the recently developed MAX–MIN ant system (MMAS) optimization [6];
2) dynamically use local and global heuristics based on the input application to adaptively search the solution space;
3) generate consistently good scheduling results over all testing cases compared with a range of list-scheduling heuristics, force-directed scheduling (FDS), simulated annealing (SA), and the optimal integer linear programming (ILP) solution, and demonstrate stable quality over a variety of application benchmarks of large size.

This paper is organized as follows: We formally define the TCS and RCS problems in Section II. In Section III, we give a brief review on the MAX–MIN ACO. Then, in Sections IV and V, we present two hybrid approaches combining traditional scheduling heuristics with the MMAS optimization to solve the TCS and RCS problems, respectively. We discuss the construction of our benchmarks in Section VI. Experimental results for the new algorithms are presented and analyzed in Section VII. In Section VIII, we compare this paper with a related study. We conclude with Section IX.

## II. Preliminaries

### A. OS Problem Definition

Given a set of operations and a collection of computational units, the RCS problem schedules the operations onto the computing units such that the execution time of these operations is minimized while respecting the capacity limits imposed by the number of computational resources. The operations can be modeled as a DFG $G(V, E)$, where each node $v_i \in V (i = 1, \ldots, n)$ represents an operation $op_i$, and the edge $e_{ij}$ denotes a dependency between operations $v_j$ and $v_i$. A DFG is a directed acyclic graph where the dependencies define a partially ordered relationship (denoted by the symbol $\preccurlyeq$) among the nodes. Without affecting the problem, we add two virtual nodes "root" and "end," which are associated with no operation (NOP). We assume that "root" is the only starting node in the DFG, i.e., it has no predecessors, and node "end" is the only exit node, i.e., it has no successors.

Additionally, we have a collection of computing resources, e.g., ALUs, adders, and multipliers. There are $R$ different types, and $r_j > 0$ gives the number of units for resource type $j$ $(1 \leqslant j \leqslant R)$. Furthermore, each operation defined in the DFG must be executable on at least one type of resource. When each of the operations is uniquely associated with one resource type, we call it "homogenous" scheduling. If an operation can be performed by more than one resource type, we call it "heterogeneous" scheduling [7]. Moreover, we assume that the cycle delays for each operation on different types of resources are known as $d(i, j)$. Of course, "root" and "end" have zero delays. Finally, we assume that the execution of the operations is non-preemptive, that is, once an operation starts execution, it must finish without being interrupted.

An RCS is given by the vector

$$\{(s_{\text{root}}, f_{\text{root}}), (s_i, f_i), \ldots, (s_{\text{end}}, f_{\text{end}})\}$$

where $s_i$ and $f_i$ indicate the starting and finishing times of the operation $op_i$. The RCS problem is formally defined as $\min(s_{\text{end}})$ with respect to the following conditions.

1) An operation can only start when all its predecessors have finished, i.e., $s_i \geqslant f_j$ if $op_j \preccurlyeq op_i$.
2) At any given cycle $t$, the number of resources needed is constrained by $r_j$ for all $1 \leqslant j \leqslant R$.

The TCS is a dual problem of the RCS version and can be defined using the same terminology presented above. Here, the target is to minimize total resources $\Sigma_j r_j$ or the total cost of the resources (e.g., the hardware area needed) subject to the same dependencies between operations imposed by the DFG and a given deadline $D$, i.e., $s_{\text{end}} < D$.

### B. Related Work

Many variants of the OS problem are $\mathcal{NP}$-hard [8]. Although it is possible to formulate and solve them using ILP [9], the feasible solution space quickly becomes intractable for larger problem instances. In order to address this problem, a range of heuristic methods with polynomial runtime complexity has been proposed.

Many TCS algorithms used in high-level synthesis are derivatives of the FDS algorithm presented in [10] and [11]. Verhaegh *et al.* [12], [13] provide a theoretical treatment on the original FDS algorithm and report better results by applying gradual time-frame reduction and the use of global spring constants in the force calculation. Due to the lack of a look-ahead scheme, the FDS algorithm is likely to produce a suboptimal solution. One way to address this issue is the iterative method proposed by Park and Kyung [14] based on Kernighan and Lin's heuristic [15] method used for solving the graph-bisection problem. In their approach, each operation is scheduled into an earlier or later step using the move that produces the maximum gain. Then, all the operations are unlocked, and the whole procedure is repeated with this new schedule. The quality of the result produced by this algorithm is highly dependent upon the initial solution. More recently, Heijligers and Jess [16] and InSyn [17] use evolutionary techniques like genetic algorithms and simulated evolution.

There are a number of algorithms for the RCS problem, including list scheduling [7], [18], FDS [10], genetic algorithm [19], tabu search [20], SA [21], and graph-theoretic and computational geometry approaches [3]. Among them, list scheduling is the most common due to its simplicity of implementation and capability of generating reasonably good results for small-sized problems. The success of the list scheduler is highly dependent on the priority function and the structure of the input application (DFG) [4], [21], [22]. One commonly used priority function assigns the priority inversely proportional to the mobility. This ensures that the scheduling of operations with large mobilities is deferred because they have more flexibility as to where they can be scheduled. Many other priority functions have been proposed [18], [19], [22], [23]. However, it is commonly agreed that there is no single good heuristic for prioritizing the DFG nodes across a range of applications using list scheduling. Our results in Section VII confirm this.

## III. ACO

Before we describe our ACOs for OS, we give a brief description of ACO metaheuristic and define terminology that we later use in our ACO formulations. Those familiar with ACO can skip or skim this section.

### A. Basic ACO

The ACO algorithm, originally introduced by Dorigo *et al.* [24], is a cooperative heuristic searching algorithm inspired by ethological studies on the behavior of ants. It was observed [25] that ants—who lack sophisticated vision—manage to establish the optimal path between their colony and a food source within a very short period of time. This is done through indirect communication known as "stigmergy" via the chemical substance, or "pheromone," left by the ants on the paths. Each individual ant makes a decision on its direction biased on the "strength" of the pheromone trails that lie before it, where a higher amount of pheromone hints a better path. As an ant traverses a path, it reinforces that path with its own pheromone. A collective autocatalytic behavior emerges as more ants will choose the shorter trails, which in turn creates an even larger amount of pheromone on those short trails, making them more likely to be chosen by future ants. The ACO algorithm is inspired by this observation. It is a population-based approach where a collection of agents cooperate together to explore the search space. They communicate via a mechanism imitating the pheromone trails.

One of the first problems to which ACO was successfully applied was the traveling salesman problem (TSP) [24], and it gave competitive results compared with traditional methods. The TSP can be modeled as a complete weighted directed graph $G = (V, E, d)$, where $V = \{1, 2, \ldots, n\}$ is a set of vertices or cities, $E = \{(i, j) | (i, j) \in V \times V\}$ is a set of edges, and $d$ is a function that associates a numeric weight $d_{ij}$ for each edge $(i, j)$ in $E$. This weight is naturally interpreted as the distance between cities $i$ and $j$. The objective is to find a Hamiltonian path for $G$ that gives the minimal length.

In order to solve the TSP problem, ACO associates a pheromone trail $\tau_{ij}$ for each edge $(i, j)$ in $E$. The pheromone indicates the attractiveness of the edge and serves as a distributed global heuristic. Initially, $\tau_{ij}$ is set with some fixed value $\tau_0$. For each iteration, $m$ ants are released randomly on the cities, and each starts to construct a tour. Every ant will have memory about the cities it has visited so far in order to guarantee the constructed tour is a Hamiltonian path. If at step $t$ the ant is at city $i$, the ant chooses the next city $j$ probabilistically using

$$\mathsf{p}_{ij} = \begin{cases} \frac{\tau_{ij}(t)^{\alpha} \cdot \eta_{ij}^{\beta}}{\Sigma_k \left(\tau_{ik}^{\alpha}(t) \cdot \eta_{ik}^{\beta}\right)}, & \text{if is } j \text{ not visited} \\ 0, & \text{otherwise} \end{cases} \tag{1}$$

where the edges $(i, k)$ are all the allowed moves from $i$, $\eta_{ik}$ is a local heuristics that is defined as the inverse of $d_{ij}$, and $\alpha$ and $\beta$ are parameters to control the relative influence of the distributed global heuristic $\tau_{ik}$ and local heuristic $\eta_{ik}$, respectively. Intuitively, the ant favors a decision on an edge

that possesses higher volume of pheromone and better local distance. At the end of each iteration, the pheromone trails are updated. More specifically, we have

$$\tau_{ij}(t) = \rho \cdot \tau_{ij}(t) + \sum_{k=1}^{m} \Delta\tau_{ij}^{k}(t), \quad \text{where } 0 < \rho < 1. \quad (2)$$

Here, $\rho$ is the evaporation ratio within the range [0,1], and $\Delta\tau_{ij}^{k} = Q/L_k$ if edge $(i, j)$ is included in the tour ant $k$ constructed, otherwise $\Delta\tau_{ij}^{k} = 0$. $Q$ is a fixed constant to control the delivery rate of the pheromone, while $L_k$ is the tour length for ant $k$. Two important operations are performed in this updating process. The evaporation operation is necessary for the ACO to be effective in exploring different parts of the search space, while the reinforcement operation ensures that frequently used edges and edges contained in the better tours receive a higher volume of pheromone and will have a better chance of being selected in the future iterations of the algorithm. The above process is repeated multiple times until a certain ending condition is reached. The best result found by the algorithm is reported.

Researchers have since formulated ACO methods for a variety of traditional $\mathcal{NP}$-hard problems. These problems include the maximum clique problem [26], the quadratic assignment problem [27], the graph coloring problem [28], the shortest common supersequence problem [29], [30], and the multiple knapsack problem [31]. ACO has also been applied to practical problems such as the vehicle routing problem [32], data mining [33], network routing problem [34], and the system-level task partitioning problem [35]–[37].

Premature convergence to local minima is a critical algorithmic issue that can be experienced by all evolutionary algorithms. Balancing exploration and exploitation is not trivial in these algorithms, especially for algorithms that use positive feedback such as ACO. This problem was formally investigated in [38]. It was shown that ACO with a time-dependent evaporation factor or a time-dependent lower-pheromone bound converges to an optimal solution with probability of exactly one. Similar to the optimality proof for the SA metaheuristic, such a global convergence guarantee can be obtained by a suitable speed of "cooling" (i.e., reduction of the influence of randomness). Although they failed in providing any constructive approach, the authors suggested that it is theoretically achievable by decreasing the evaporation factors or by slowly decreasing the lower-pheromone bounds.

### B. MMAS

MMAS [6] is built upon the original ACO algorithm and is specifically designed to address the premature convergence problem. It improves the original ACO by providing dynamically evolving bounds on the pheromone trails such that the heuristic value is always within a limit to that of the best path. As a result, all possible paths will have a nontrivial probability of being selected and thus encourages broader exploration of the search space.

More specifically, MMAS forces the pheromone trails to be limited within evolving bounds, that is, for iteration $t$, $\tau_{\min}(t) \leqslant \tau_{ij}(t) \leqslant \tau_{\max}(t)$. If we use $f$ to denote the cost function of a specific solution $S$, the upper bound $\tau_{\max}$ [6] is shown as

$$\tau_{\max}(t) = \frac{1}{1-\rho} \frac{1}{f\left(S^{\mathrm{gb}}(t-1)\right)} \quad (3)$$

where $S^{\mathrm{gb}}(\cdot)$ represents the global best solution found so far in all iterations. The lower bound is defined as

$$\tau_{\min}(t) = \frac{\tau_{\max}(t)(1 - \sqrt[n]{p_{\mathrm{best}}})}{(avg-1)\sqrt[n]{p_{\mathrm{best}}}} \quad (4)$$

where $p_{\mathrm{best}} \in (0, 1]$ is a controlling parameter to dynamically adjust the bounds of the pheromone trails. The physical meaning of $p_{\mathrm{best}}$ is that it indicates the conditional probability of the current global best solution $S^{\mathrm{gb}}(t)$ being selected given that all edges not belonging to the global best solution have a pheromone level of $\tau_{\min}(t)$, and all edges in the global best solution have $\tau_{\max}(t)$. Here, $avg$ is the average size of the decision choices over all the iterations. For a TSP problem of $n$ cities, $avg = n/2$. It is noted from (4) that lowering $p_{\mathrm{best}}$ will result in a tighter range for the pheromone heuristic. As $p_{\mathrm{best}} \to 0$, $\tau_{\min}(t) \to \tau_{\max}(t)$, which means more emphasis is given to search space exploration.

Theoretical treatments of using pheromone bounds and other modifications on the original ACO algorithm are proposed in [6]. These include a pheromone-updating policy that only utilizes the best performing ant, initializing pheromone with $\tau_{\max}$, and combining local search with the algorithm. It was reported that MMAS was the best performing ACO approach and provided very high quality solutions.

## IV. MMAS FOR TCS

In this section, we introduce our MMAS-based algorithms for solving the TCS problem. As discussed in Section II, FDS is a commonly used heuristic as it generates "good" quality results for moderately sized DFGs. Our algorithm uses distribution graphs from FDS as a local heuristic. Additionally, we use the results produced by FDS to evaluate the quality of our algorithm. For these reasons, we provide some details of FDS in the following subsection. The remaining subsections describe our MMAS algorithm for TCS.

### A. FDS

The FDS algorithm (and its various forms) has been widely used since it was first proposed by Paulin and Knight [10]. The goal of the algorithm is to reduce the number of functional units used in the implementation of the design. This objective is achieved by attempting to uniformly distribute the operations onto the available resource units. The distribution ensures that resource units allocated to perform operations in one control step are used efficiently in all other control steps, which leads to a high utilization rate.

The FDS algorithm relies on both the as-soon-as-possible (ASAP) and the as-late-as-possible (ALAP) scheduling algorithms to determine the feasible control steps for every operation $op_i$ or the time frame of $op_i$ (denoted as $[t_i^S, t_i^L]$, where

$t_i^S$ and $t_i^L$ are the ASAP and ALAP times, respectively). It also assumes that each operation $op_i$ has a uniform probability of being scheduled into any of the control steps in the range and zero probability of being scheduled elsewhere. Thus, for a given time step $j$ and an operation $op_i$ that needs $\triangle_i \geqslant 1$ time steps to execute, this probability is given as

$$\mathsf{p}_j(op_i) = \begin{cases} \left(\sum_{l=0}^{\triangle_i} h_i(j-l)\right) \Big/ \left(t_i^L - t_i^S + 1\right), & \text{if } t_i^S \leqslant j \leqslant t_i^L \\ 0, & \text{otherwise} \end{cases} \quad (5)$$

where $h_i(\cdot)$ is a unit window function defined on $[t_i^S, t_i^L]$.

Based on this probability, a set of distribution graphs can be created, one for each specific type of operation, denoted as $q_k$. More specifically, for type $k$ at time step $j$, we have

$$q_k(j) = \sum_{op_i} \mathsf{p}_j(op_i), \quad \text{if the type of } op_i \text{ is } k. \quad (6)$$

We can see that $q_k(j)$ is an estimation on the number of type-$k$ resources that are needed at control step $j$.

The FDS algorithm tries to minimize the overall concurrency under a fixed latency by scheduling operations one by one. At every time step, the effect of scheduling each unscheduled operation on every possible time step in its frame range is calculated, and the operation and the corresponding time step with the smallest negative effect are selected. This effect is equated as the force for an unscheduled operation $op_i$ at control step $j$ and is comprised of two components, namely: 1) the self-force $SF_{ij}$ and 2) the predecessor–successor forces $PSF_{ij}$.

The self-force $SF_{ij}$ represents the direct effect of this scheduling on the overall concurrency. It is given by

$$SF_{ij} = \sum_{l=t_i^S}^{t_i^L+\triangle_i} q_k(l)\left(H_i(l) - \mathsf{p}_i(l)\right) \quad (7)$$

where $j \in [t_i^S, t_i^L]$, $k$ is the type of operation $op_i$, and $H_i(\cdot)$ is the unit window function defined on $[j, j+\triangle_i]$.

We also need to consider the predecessor and successor forces since assigning operation $op_i$ to time step $j$ might cause the time frame of a predecessor or successor operation $op_l$ to change from $[t_l^S, t_l^L]$ to $[\widetilde{t}_l^S, \widetilde{t}_l^S]$. The force exerted by a predecessor or successor is given by

$$PSF_{ij}(l) = \sum_{m=\widetilde{t}_i^S}^{\widetilde{t}_i^L+\triangle_l} \left(q_k(m)\cdot \widetilde{\mathsf{p}}_m(op_l)\right) - \sum_{m=t_i^S}^{t_i^L+\triangle_l} \left(q_k(m)\cdot \mathsf{p}_m(op_l)\right) \quad (8)$$

where $\widetilde{\mathsf{p}}_m(op_l)$ is computed in the same way as (5) except the updated mobility information $[\widetilde{t}_l^S, \widetilde{t}_l^S]$ is used. Notice that the above computation has to be carried for all the predecessor and successor operations of $op_i$. The total force of the hypothetical assignment of scheduling $op_i$ on time step $j$ is the addition of the self-force and all the predecessor–successor forces, i.e.,

$$\text{total force}_{ij} = SF_{ij} + \sum_l PSF_{ij}(l) \quad (9)$$

where $op_l$ is a predecessor or successor of $op_i$. Finally, the total forces obtained for all the unscheduled operations at every possible time step are compared. The operation and time step with the best force reduction are chosen, and the partial scheduling result is incremented until all the operations have been scheduled.

The FDS method is "constructive" because the solution is computed without performing any backtracking. Every decision is made in a greedy manner. If there are two possible assignments sharing the same cost, the above algorithm cannot accurately estimate the best choice. Based on our experience, this happens fairly often as the DFG becomes larger and more complex. Moreover, FDS does not take into account future assignments of operators to the same control step. Consequently, it is likely that the resulting solution will not be optimal due to the lack of a look-ahead scheme and the lack of compromises between early and late decisions.

Our experiments show that a baseline FDS implementation based on [10] fails to find the optimal solution even on small testing cases. To ease this problem, a look-ahead factor was introduced in the same paper. A second-order term of the displacement weighted by a constant $\eta$ is included in force computation, and the value $\eta$ is experimentally decided to be 1/3. In our experiments, this look-ahead factor has a positive impact on some testing cases but does not always work well. More details regarding FDS performance can be found in Section VII.

### B. MMAS for TCS

We address the TCS problem in an evolutionary manner. The proposed algorithm is built upon the ant system approach, and the TCS problem is formulated as an iterative searching process. Each iteration consists of two stages. First, the ACO algorithm is applied in which a collection of ants traverse the DFG to construct individual operation schedules with respect to the specified deadline using global and local heuristics. Second, these results are evaluated using their resource costs. The heuristics are adjusted based on the solutions found in the current iteration. The hope is that future iterations will benefit from this adjustment and come up with better schedules.

Each operation or DFG node $op_i$ is associated with $D$ pheromone trails $\tau_{ij}$, where $j = 1, \ldots, D$, and $D$ is the specified deadline. These pheromone trails indicate the global favorableness of assigning the $i$th operation at the $j$th control step in order to minimize the resource cost with respect to the time constraint. Initially, based on ASAP and ALAP results, $\tau_{ij}$ is set with some fixed value $\tau_0$ if $j$ is a valid control step for $op_i$; otherwise, it is set to be 0.

For each iteration, $m$ ants are released, and each ant individually starts to construct a schedule by picking an unscheduled operation and determining its desired control step. However,

unlike the deterministic approach used in the FDS method, each ant picks up the next operation probabilistically. The simplest way is to select an operation uniformly among all unscheduled operations. Once an operation $op_h$ is selected, the ant needs to make a decision on which control step it should be assigned to. This decision is also made probabilistically according to

$$\mathsf{p}_{hj} = \begin{cases} \frac{\tau_{hj}(t)^{\alpha} \cdot \eta_{hj}^{\beta}}{\sum_l (\tau_{hl}^{\alpha}(t) \cdot \eta_{hl}^{\beta})}, & \text{if } op_h \text{ can be scheduled at } l \text{ and } j \\ 0, & \text{otherwise} \end{cases}. \tag{10}$$

Here, $j$ is the control step under consideration, which is between $op_h$'s time frame $[t_h^S, t_h^L]$. The item $\eta_{hj}$ is the local heuristic for scheduling operation $op_h$ at control step $j$, and $\alpha$ and $\beta$ are parameters to control the relative influence of the distributed global heuristic $\tau_{hj}$ and local heuristic $\eta_{hj}$, respectively. In this paper, assuming $op_h$ is of type $k$, we simply set $\eta_{hj}$ to be the inverse of $q_k(j)$, that is, the distribution graph value of type $k$ at control step $j$ (calculated in the same way as in FDS). Recalling our discussion in Section IV-A, $q_k$ is computed based on partial scheduling result and is an indication on the number of computing units of type $k$ needed at control step $j$. Intuitively, the ant favors a decision that possesses higher volume of pheromone and better local heuristic, i.e., a lower $q_k$. In other words, an ant is more likely to make a decision that is globally considered "good" and also uses the fewest number of resources under the current partially scheduled result. Similar to FDS, once an operation is fixed at a time step, it will not change. Furthermore, the time frames will be updated to reflect the changed partial schedule. This guarantees that each ant will always construct a valid schedule.

In the second stage of our algorithm, the ant's solutions are evaluated. The quality of the solution from ant $h$ is judged by the total number of resources, i.e., $Q_h = \Sigma_k r_k$. At the end of the iteration, the pheromone trail is updated according to the quality of individual schedules. Additionally, a certain amount of pheromone evaporates. More specifically, we have

$$\tau_{ij}(t) = \rho \cdot \tau_{ij}(t) + \sum_{h=1}^{m} \Delta\tau_{ij}^{h}(t), \quad \text{where } 0 < \rho < 1. \tag{11}$$

Here, $\rho$ is the evaporation ratio, and

$$\Delta\tau_{ij}^{h} = \begin{cases} Q/Q_h, & \text{if } op_i \text{ is scheduled at } j \text{ by ant } h \\ 0, & \text{otherwise} \end{cases}. \tag{12}$$

$Q$ is a fixed constant to control the delivery rate of the pheromone. Two important operations are performed in the pheromone trail updating process. Evaporation is necessary for ACO to effectively explore the solution space, while reinforcement ensures that the favorable operation orderings receive a higher volume of pheromone and will have a better chance of being selected in the future iterations. The above process is repeated multiple times until an ending condition is reached. The best result found by the algorithm is reported.

In our experiments, we implemented both the basic ACO and the MMAS algorithms. The latter consistently achieves better scheduling results, especially for larger DFGs. A pseudocode implementation of the final version of our TCS algorithm using MMAS is shown as Algorithm 1, where the pheromone bounding step is indicated as step 23.

**Algorithm 1**: MMAS for TCS
**procedure** MaxMinAntSchedulingTCS($G$, $R$)
**input**: DFG $G(V, E)$, resource set $R$
**output**: operation schedule
1. initialize parameter $\rho, \tau_{ij}, p_{\text{best}}, \tau_{\max}, \tau_{\min}$
2. construct $m$ ants
3. $BestSolution \leftarrow \phi$
4. **while** ending condition is not met **do**
5. **for** $i = 0$ **to** $m$ **do**
6. $ant(i)$ constructs a valid schedule timing constrained $S_{current}$ as following:
7. $S_{current} \leftarrow \phi$
8. perform ASAP and ALAP
9. **while** exists unscheduled operation **do**
10. update time frame $[t_i^S, t_i^L]$ associated with each operation $op_i$ and the distribution graphs $q_k$.
11. select one operation $op_h$ among all unscheduled operations probabilistically
12. **for** $t_h^S \leqslant j \leqslant t_h^L$ **do**
13. set local heuristic $\eta_{hj} = 1/q_k(j)$ where $op_h$ is of type $k$
14. **end for**
15. select time step $l$ using $\eta$ and $\tau$ as (10).
16. $S_{current} = schedule(S_{current}, op_h, l)$
17. Update time frame and distribution graphs based on $S_{current}$
18. **end while**
19. **if** $S_{current}$ is better than that of $BestSolution$} **then**
20. $BestSolution \leftarrow S_{current}$
21. **end if**
22. **end for**
23. update $\tau_{\max}$ and $\tau_{\min}$ based on (3) and (4)
24. **update** $\eta$ **if needed**
25. update $\tau_{ij}$ based on (11)
26. **end while**
27. return $BestSolution$

### C. Refinements

*1) Updating Neighboring Pheromone Trails:* We found that a "better" solution can often be achieved from a "good" scheduling result by simply adjusting very few operations' scheduled positions within their time frames. Based on this observation, we can refine our pheromone update policy to encourage exploration of the neighboring positions. More specifically, in the pheromone reinforcement step indicated by (12), we also increase the pheromone trails of the control steps' adjacent position $j$ subject to a weighted function window. Two such windowing functions are shown in Fig. 2. Depending on the neighbor's offset from $j$, the two functions adjust its pheromone trail in a similar manner to (12) but with an extra factor applied. Assuming we use $x$ to represent the offset, then Fig. 2(a) has a weight function of $1 - 1/3|x|$, while Fig. 2(b) provides a weight function of $e^{-|x|}$. In our experiments, the

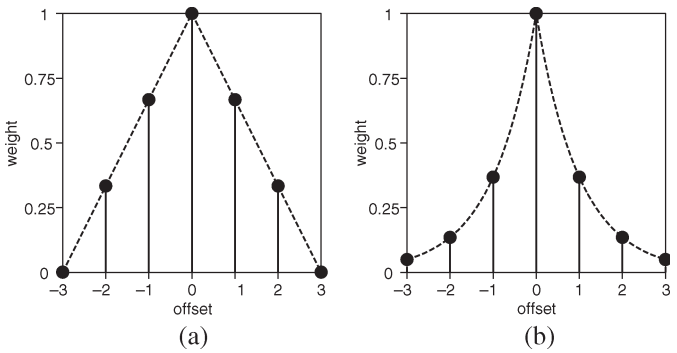


Fig. 2. Pheromone update windows.

latter provides relatively better performance. Ideally, the weight function window size shall be computed based on the mobility ranges of the operations. However, to keep the algorithm simple, we use a window size 5 across all our experiments, subject to the operation's time frame $[t_i^S, t_i^L]$. This number is estimated using the average mobility ranges of all testing cases.

*2) Operation Selection:* In our algorithm, the ants construct a schedule for the given DFG by making two decisions in sequence. First, it needs to select the next operation. Then, a specific control step is determined for the selected operation. As discussed earlier, the simplest approach for selecting an operation is to randomly pick one among all the unscheduled operations. Although it is simple and computationally effective, it does not appreciate the information accumulated in the pheromone from the previous iterations; it also ignores the dynamic time-frame information. One possible refinement is to make the selection probability proportional to the pheromone and inversely proportional to the size of the operation's time frame at that instance. More precisely, we pick the next operation $op_i$ probabilistically with

$$\mathsf{p}_i = \frac{\frac{\sum_j \tau_{ij}}{\left(t_i^L - t_i^S + 1\right)}}{\sum_l \frac{\sum_k \tau_{lk}}{\left(t_l^L - t_l^S + 1\right)}}. \tag{13}$$

Here, the numerator can be viewed as the average pheromone value over all possible positions in the current time frame for operation $op_i$. The denominator is a normalization factor to bring the result to a valid probability value between 0 and 1. It is basically the addition of the average pheromone for all the unscheduled operations $op_l$. Notice that as the time frames of the operations change dynamically depending on the partial schedule, the average pheromone trail is not constant during the schedule construction process. In other words, we only consider a pheromone $\tau_{ij}$ when $t_i^S \leqslant j \leqslant t_i^L$.

Intuitively, this formulation favors an operation with stronger pheromone and fewer possible scheduling alternatives. In the extreme case, $t_i^L = t_i^S$, which means operation $op_i$ is on the critical path, we will have only one choice for $op_i$. If the pheromone for $op_i$ at this position happens to be very strong, we will have better chance to pick $op_i$ at the next step compared with other operations. Our experiments show that applying this operation selection policy makes the algorithm faster in identifying high-quality results. Compared with the even possibility approach, there is an overhead in performing this operation selection policy. However, by making the selection more targeted, it allows us to reduce the overall iteration number of the algorithm; thus, the additional overhead is well worth it. In our experiments, we were able to reduce the total runtime by about 23% while achieving almost the same quality with our testing results by adopting this biased selection policy.

### D. Extensions

Our proposed TCS algorithm applies the ACO metaheuristic at the high level. It poses little difficulty to extend it to handle different scheduling contexts. Most of the methods proposed previously for FDS can be readily implemented within our framework.

*1) Resource Preference:* In this paper, the target is to minimize the total count of resources needed. Accordingly, we use the inverse of this total count as the quality of the scheduling result. This quality measurement is further used to adjust the pheromone trails. However, in practice, we may have unbalanced hardware costs for different resource types. With this consideration, we might find that we prefer a schedule that requires three multipliers and four adders rather than one that needs four multipliers and three adders, although both schedules have the same total number (i.e., seven) of resources. This issue can be handled in our algorithm simply by introducing a cost factor $c_k$ for each resource type and modifying the quality of the schedule to this weighted resource cost, i.e.,

$$Q_h = \sum_k (c_k r_k). \tag{14}$$

By adjusting the $c_k$ assigned to different resource types, we can control the preference in our schedule results.

*2) Multicycle Operation:* No change is needed for our algorithm to handle multicycle operation since it uses dynamically computed time frames. Also, as presented in Section IV-A, the distribution graph handles multicycle operations naturally.

*3) Mutually Exclusive Operations:* Mutually exclusive operations occur when operations are located in different branches of the program. This happens in "if–then–else" and "case" statements in high-level languages. With the proposed algorithm, we do not need to add any extra constraint for handling such operations; thus, the approach proposed in [10] is still valid.

*4) Chained Operations:* When the total delay of consecutive operations is less than a clock cycle, it is possible to chain the operations during scheduling. The same techniques used in [10] can be directly applied within our approach, where chaining is handled by extending the ASAP and ALAP computation to obtain the time frames for the operations.

*5) Pipelining:* For pipelined resources, there exists additional parallelism provided by functional pipelining. Here, optimizing an individual control step becomes inappropriate and limited. We have to consider scheduling optimization over groups of control steps. We can solve this by slicing and superimposing the distribution graph in a manner depending on the latency [10]. Again, this method can also be applied to extend our algorithm to handle the pipelined scenario.

### *E. Complexity Analysis*

As we can see, the construction of an individual schedule by the ants, or the body of the inner loop in the proposed algorithm, is of complexity $O(n^2)$, where $n$ is the number of nodes in the DFG under consideration. Thus, the total complexity of the algorithm is determined by the number of ants $m$ and the iteration number $N$. Theoretically, the production of $m$ and $N$ shall be proportional to the production of $n$ and the deadline $D$. In this case, we have a total complexity of $O(Dn^3)$, which is the same as the unoptimized version of FDS. However, in practice, we found it is possible to fix $m$ and $N$ for a large range of applications (see Section VII). This means that in practical use the algorithm can be expected to work with $O(n^2)$ complexity for most of the cases.

## V. MMAS FOR RCS

In this section, we present our algorithm of applying the ant system heuristic, or more specifically the MMAS [6], for solving the OS problem under resource constraints.

### *A. Algorithm Formulation*

As discussed in Section II, list scheduling is the most widely used method for the RCS problem. A list scheduler takes a DFG and a priority list of all the nodes in the DFG as input. The list is sorted with decreasing magnitude of priority assigned to each of the operations. The list scheduler maintains a ready list, i.e., nodes whose predecessors have already been scheduled. In each iteration, the algorithm scans the priority list, and operations with higher priority are scheduled first. Scheduling an operator to a control step makes its successor operations ready, which will be added to the ready list. This process is repeated until all of the operations have been scheduled. When there exist more than one ready operations sharing the same priority, ties are broken randomly. The effectiveness of the list scheduler heavily depends on the priority list. Although there exist many different heuristics on how to order the list, it is commonly believed that the best list depends on the structure of the input application. A priority list based on a single heuristic limits the exploration of the search space for the list scheduler.

Based on this observation, we address the RCS problem in a similar manner to the ACO metaheuristic framework used to solve the TCS problem. The key idea is to combine the ACO metaheuristic with the traditional list-scheduling algorithm and formulate the problem as an iterative searching process over the operation list space.

Similar to the algorithm formulated for the TCS problem, each operation, or DFG node $op_i$, is associated with a set of pheromone trails $\tau_{ij}$. The difference is that now each trail indicates the global favorableness of assigning the $i$th operation at the $j$th position in the priority list, where $j = 1, \ldots, n$. Since it is valid for the operation to be assigned to any of the position in the priority list, each pheromone trail will be valid. This is different from the TCS formulation where some trails are fixed to be zero based on the allowed time frames of the operations. Initially, $\tau_{ij}$ is set with some fixed value $\tau_0$.

A pseudocode implementation of our RCS algorithm using MMAS is shown in Algorithm 2, where the pheromone bounding step is indicated as step 12.

**Algorithm 2**: MMAS for RCS
**procedure** MaxMinAntSchedulingRCS$(G, R)$
**input**: DFG $G(V, E)$, resource set $R$
**output**: operation schedule
1. initialize parameter $\rho, \tau_{ij}, p_{\text{best}}, \tau_{\max}, \tau_{\min}$
2. construct $m$ ants
3. $BestSolution \leftarrow \phi$
4. while ending condition is not met}
5. **for** $i = 0$ **to** $m$ **do**
6. $ant(i)$ constructs a list $L(i)$ of nodes using $\tau$ and $\eta$
7. $Q_i =$ ListScheduling$(G, R, L(i))$
8. **if** $Q_i$ is better than that of $BestSolution$}
9. $BestSolution \leftarrow L(i)$
10. **end if**
11. **end for**
12. update $\tau_{\max}$ and $\tau_{\min}$ based on (3) and (4)
13. **update** $\eta$ **if needed**
14. update $\tau_{ij}$ based on (11)
15. **end while**
16. return $BestSolution$

For each iteration, $m$ ants are released, and each starts to construct an individual priority list by filling the list with one operation per step. Every ant will have memory about the operations it has already selected in order to guarantee the validity of the constructed list. Upon starting step $j$, the ant has already selected $j-1$ operations of the DFG. To fill the $j$th position of the list, the ant chooses the next operation $op_i$ probabilistically according to

$$\mathsf{p}_{ij} = \begin{cases} \dfrac{\tau_{ij}(t)^{\alpha} \cdot \eta_{ij}^{\beta}}{\sum_k \left(\tau_{kj}^{\alpha}(t) \cdot \eta_{kj}^{\beta}\right)}, & \text{if } op_k \text{ is not scheduled yet} \\ 0, & \text{otherwise} \end{cases} \tag{15}$$

where the eligible operations $op_k$ are those yet to be scheduled. Again, $\eta_{ik}$ is a local heuristic for selecting operation $op_k$, and $\alpha$ and $\beta$ are parameters to control the relative influence of the distributed global heuristic $\tau_{ik}$ and local heuristic $\eta_{ik}$, respectively.

The local heuristic $\eta$ gives the local favorableness of scheduling the $i$th operation at the $j$th position of the priority list. In this paper, we experimented with different well-known heuristics [4] proposed for OS.

1) Operation mobility (OM): The mobility of an operation gives the range for scheduling the operation. It is computed as the difference between ALAP and ASAP results. The smaller is the mobility, the more urgent is the scheduling of the operation. When the mobility is zero, the operation is on the critical path.
2) Operation depth (OD): OD is the length of the longest path in the DFG from the operation to the sink. It is an obvious measure for the priority of an operation as it gives the number of operations we must pass.

3) Latency-weighed OD (LWOD): LWOD is computed in a similar manner as OD except that the nodes along the path are weighed using their operation latencies.
4) Successor number (SN): The motivation of using the number of successors is the hope that scheduling a node with more successors has a higher possibility of making other nodes in the DFG free, thus increasing the number of possible operations to choose from later on.

The second stage of the algorithm, i.e., the result quality assessment and pheromone trail updating, proceeds similarly as the TCS algorithm discussed previously. The only exception is that now the quality $Q_h$ in (12) is replaced by the total latency $L_h$ of the generated scheduling result.

### B. Refinements

*1) Dynamic Local Heuristics:* One important difference between our algorithm and other ant system algorithms is that we use a dynamic local heuristic in the RCS process. It is indicated by step 13 in Algorithm 2. This technique allows better local guidance to the ants for making the selection in the next iteration. We will illustrate this feature with the use of the OM heuristic.

Typically, the mobility of an operation is computed by using ALAP and ASAP results. One important input parameter in computing the ALAP result is the estimated scheduling deadline. This deadline is usually obtained from system specifications or other quick heuristic methods such as a list scheduler. It is clear that more accurate deadline estimations will yield a tighter mobility range, thus better local guidance.

Based on the above observation, we use dynamically computed mobility as the local heuristic in our algorithm. As the algorithm proceeds, whenever a better schedule is achieved, we use the newly obtained scheduling length as the deadline for computing the ALAP result for the next iteration. That is, for iteration $t$, the local heuristic for operation $i$ is computed as (see Section III-B for definitions for $f$ and $S^{\mathrm{gb}}$)

$$\eta_i(t) = \frac{1}{\mathrm{ALAP}\left(f\left(S^{\mathrm{gb}}(t-1)\right), i\right) - \mathrm{ASAP}(i) + 1}. \quad (16)$$

*2) Topologically Sorted Lists:* In the above algorithm, the ants construct a priority list using the same traversing method that is used in the TSP formulation [24]. In fact, this turns out to be a naive way. To illustrate this, one just needs to notice that it will yield a search space of totally $n!$ possible lists, which is simply all the permutations of $n$ operations. However, we know that the resultant schedules of the list scheduler are only a small portion of these lists. More precisely, they are all the possible permutations of the operations that are topologically sorted based on the dependency constraints imposed by the DFG. By leveraging this application-dependent feature, it is possible for us to greatly reduce the search space. For instance, using this technique on a simple 11-node example [4] reduces the possible number of orderings from 11! to 59 400, or 0.15%. Although it quickly becomes prohibitive to precisely compute such reduction for more complex graphs,[1] it is generally significant. By adopting this technique, in the final version of our algorithm, the ant traverses the DFG in a similar manner to the list-scheduling process and fills the operation list one by one. At each step, the ant will select an operation based on (15) but only from all the ready operations, that is, from all the operations whose predecessors have all been scheduled.

### C. Extensions

So far, our discussion on the OS problems has been limited to the "homogeneous" case. In other words, each operation is mapped to a unique resource type, although a resource type might be able to handle different operations. In practice, this means that a "resource allocation" step needs to precede the OS process. We often need to handle the "heterogeneous" case, where one operation can be executed with different resource types. For example, a system might have two different realizations of multiplier: one is faster but more expensive, while the other is slower but cheaper. Both are capable of executing a multiplication operation. Our challenge is to determine how to effectively use the resources to achieve the best time performance. In this situation, separating the resource allocation step from OS may not be a favorable approach, as the prior step could greatly limit the optimization opportunity for OS. This motivates us to consider the resource allocation issue within the OS problem.

It is possible to address this problem using ILP by extending the ILP formulation for the homogenous case. The basic idea is to introduce a new set of parameters $m_{ik}$ that can take the value of 0 or 1 and describe the compatibility between operation $op_i$ and resource type $k$. A set of new constraints is needed to make sure that only one type of resource among all those that are capable of processing $op_i$ is used, i.e.,

$$\sum_k m_{ik} = 1, \quad \text{where } i = 1, \ldots, n. \quad (17)$$

We can see that it makes the ILP problem even more intractable.

However, this extra difficulty does not block the list scheduler or the proposed MMAS approach from working. The basic algorithm could be carried out with almost no changes except for the list construction. The major problem is that, when there exist alternative resource types for one specific operation, estimating a certain attribute of the operation becomes more challenging. For example, with different execution delay on capable resource types, the mobility of the operation is variable. This has been studied in previous research, e.g., [7], where the average latency over a set of heterogeneous resources is used to carry the scheduling task. In this paper, we simply take the pessimistic approach by applying the longest execution latency among the alternative resources in computing such attributes. With this extension, our algorithm can be applied to heterogeneous cases.

[1] We tried to compute the search space reduction for Fig. 5 using GenLE [39]. It failed to produce any result within 100 computer hours.

### D. Complexity Analysis

List scheduling is a two-step process. In the first step, a priority list is built. The second step takes $n$ steps to solve the scheduling problem since it is a constructive method without backtracking. For different heuristics, the complexity of the first step is different. When OM, OD, and LWOD are used, it takes $O(n^2)$ steps to build the priority list since a depth-first or breadth-first graph transverse is involved. When the successor node number is adopted as the list construction heuristic, it only takes $n$ step. Thus, the complexities for these methods are $O(n^2)$ or $O(n)$.

The force-directed RCS method is different. Although it is also a constructive method without backtracking, we need to compute the force of each operation at every step since the total latency is dynamically increased based on whether there is enough resources to handle the ready operations. Thus, the FDS method has $O(n^3)$ complexity.

The complexity of the proposed MMAS solution is determined mainly by the complexity of constructing individual scheduling solutions, the number of ants $m$, and the total iteration $N$ in every run. In order to generate a schedule solution, each ant needs to first loop through $n$ operations and for each operation determine its location, which has a complexity of $O(n)$. This list is then provided to a list scheduler with a complexity of $O(n)$ or $O(n^2)$. This makes an overall complexity of $O(n^2)$. Obviously, if $mN$ is proportional to $n$, we will have one-order higher complexity than the corresponding list-scheduling approach. However, based on our experience, it is possible to fix such factor for a large set of practical cases so that the complexity of the MMAS solution is the same as the list-scheduling approach.

## VI. Benchmarks

In order to test and evaluate our algorithms, we have constructed a comprehensive set of benchmarks. These benchmarks are taken from one of two sources:

1) popular benchmarks used in the previous literature;
2) real-life examples generated and selected from the MediaBench suite [40].

The benefit of having classic samples is that they provide a direct comparison between results generated by our algorithm and that from previously published methods. This is especially helpful when some of the benchmarks have known optimal solutions. In our final testing benchmark set, seven samples widely used in OS studies are included. These samples focus mainly on frequently used numeric calculations performed by different applications. They are listed as follows.

1) ARF: an implementation of an "autoregression filter."
2) EWF: an implementation of an "elliptic wave filter."
3) FIR1 and FIR2: two versions of a "finite impulse response filter."
4) COSINE1 and COSINE2: two implementations for a 1-D eight-point fast DCT, where COSINE1 assumes constant coefficients while the coefficients in COSINE2 are given as inputs.
5) HAL: an iterative solution of a second-order differential equation. This perhaps is the most popularly used example in textbooks that originally appeared in [10].

However, these samples are typically small to medium in size and are considered somewhat old. To be representative, it is necessary to create a more comprehensive set with benchmarks of different sizes and complexities. Such benchmarks shall aim to the following:

1) provide real-life testing cases from real-life applications;
2) provide more up-to-date testing cases from modern applications;
3) provide challenging samples for OS algorithms with regards to larger number of operations, higher level of parallelism, and data dependency;
4) provide a wide range of synthesis problems to test the algorithms' scalability.

For this purpose, we have investigated the MediaBench suite, which contains a wide range of complete applications for image processing, communications, and DSP applications. We analyzed these applications using SUIF [41] and Machine SUIF [42] tools, and over 14 000 DFGs were extracted as preliminary candidates for our benchmark set. After careful study, 13 DFG samples were selected from four MediaBench applications. These applications are listed as follows.

1) JPEG: JPEG is a lossy compression technique for digital images. The "cjpeg" application performs compression, while the "djpeg" application decompresses the JPEG image.
2) MPEG2: MPEG2 is a digital video compression standard commonly used for high-quality video compression including DVD compression. The mpeg2enc application encodes the video, while the mpeg2dec application decodes the video.
3) EPIC: EPIC stands for efficient pyramid image coder and is another image compression utility.
4) MESA: The Mesa project is a software 3-D graphics package. The primary application that we were concerned with was the "texgen" utility, which generates a texture-mapped version of the Utah teapot.

From the JPEG project, four basic blocks were selected. The first came from the write_bmp_header function. The basic block was selected for its high level of parallelism. The second basic block came from the h2v2_smooth_downsample function. This function has 51 nodes for only one store operation at the end. The store is dependent on all but two of the operations, making it an interesting problem for scheduling. The third basic block was selected from the jpeg_fdct_islow function. The function performs an integer forward DCT using a slow-but-accurate algorithm and was chosen for its popularity among DSP applications. The final block was selected from the jpeg_idct_ifast function. Like the forward DCT, this was selected for its commonality. However, this implementation is a fast, and much less accurate, version of the inverse DCT.

Two basic blocks were selected from the MPEG section. The first came from the "idctcol" function in the "mpeg2dec" application. The function implements another version of the inverse DCT algorithm. In this case, the function is part of a 2-D

TABLE I
BENCHMARK NODE AND EDGE COUNT WITH OD ASSUMING UNIT DELAY

| *Benchmark Name* | *# Nodes* | *# Edges* | *OD* |
|---|---|---|---|
| HAL | 11 | 8 | 4 |
| horner_bezier | 18 | 16 | 8 |
| ARF | 28 | 30 | 8 |
| motion_vectors | 32 | 29 | 6 |
| EWF | 34 | 47 | 14 |
| FIR2 | 40 | 39 | 11 |
| FIR1 | 44 | 43 | 11 |
| h2v2_smooth_downsample | 51 | 52 | 16 |
| feedback_points | 53 | 50 | 7 |
| collapse_pyr | 56 | 73 | 7 |
| COSINE1 | 66 | 76 | 8 |
| COSINE2 | 82 | 91 | 8 |
| write_bmp_header | 106 | 88 | 7 |
| interpolate_aux | 108 | 104 | 8 |
| matmul | 109 | 116 | 9 |
| idctcol | 114 | 164 | 16 |
| jpeg_idct_ifast | 122 | 162 | 14 |
| jpeg_fdct_islow | 134 | 169 | 13 |
| smooth_color_z_triangle | 197 | 196 | 11 |
| invert_matrix_general | 333 | 354 | 11 |

inverse DCT, while the inverse DCT from the JPEG application is only 1-D. The large size of the DFG and the complicated dependency structure provide a good test for the scheduling algorithm. The second comes from the motion_vectors function in the "mpeg2enc" function. The basic block only contains 42 nodes and 38 edges, making it one of the smaller blocks selected from MediaBench, ensuring that the benchmark suite provides a wide range of synthesis problems to test scalability.

The EPIC project supplied one basic block. It came from the collapse_pyr function, which is a quadrature mirror filter bank. The block was selected for its medium size and common use in DSP applications.

From the MESA application, six basic blocks were selected to be added to the benchmark suite. The invert_matrix_general and "matmul" functions were selected because they are general functions, not specific to the MESA application. Matrix operations, such as inversion and multiplication, are common in DSP applications where many filters are merely matrix multiplications with a set of coefficients. The next block selected came from the smooth_color_z_triangle function. The basic block is essentially four parallel computations without data dependencies, making it an ideal addition to the benchmark suite. The fourth benchmark is from the horner_bezier method. With only 18 nodes, the small size helps add variety to the benchmarks. The fifth block comes from the interpolate_aux function. The function performs four linear interpolation calculations, which can easily be run in parallel if the hardware is available. The final benchmark is from the feedback_points function, which calculates texture coordinates for a feedback buffer.

Table I lists all 20 benchmarks that were included in our final benchmark set, together with the names of the various functions where the basic blocks originated are the number of nodes, number of edges, and OD (assuming unit delay for every operation) of the DFG. The data, including related statistics, DFG graphs, and source code for the all testing benchmarks, are available online [43].

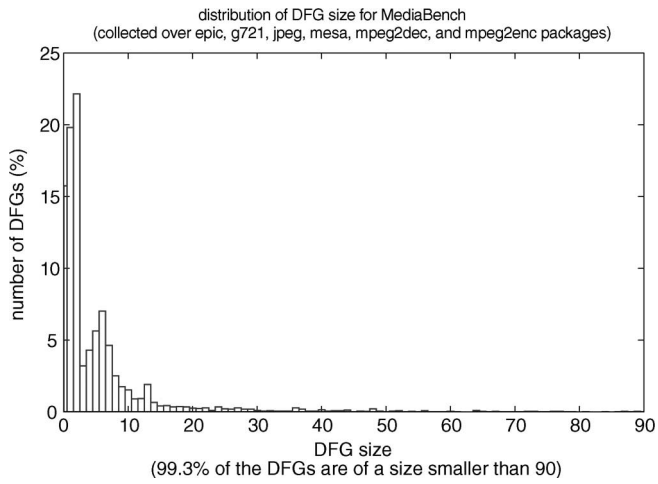


Fig. 3. Distribution of DFG size for MediaBench.

In order to justify the difficulty and representativeness of our testing cases, we analyze the distribution of the sizes of DFGs in practical software programs. Our analysis covers the "epic," "jpeg," "g721," "mpeg2enc," "mpeg2dec," and "mesa" packages. The result is shown in Fig. 3. We found that the maximum size of a DFG can be as big as 632. However, the majority of the DFGs are much smaller. In fact, more than 99.3% DFGs have fewer than 90 nodes. Moreover, the very largest ones are of little interest with respect to system performance. They are typically related to system initialization and are executed only once.

## VII. EXPERIMENTAL RESULTS

### A. TCS

In order to evaluate the quality of our proposed algorithm for the TCS problem, we compare its results with that obtained by the widely used FDS method. For all testing benchmarks, operations are allocated on two types of computing resources, namely MUL and ALU, where MUL is capable of handling multiplication and division, and ALU is used for other operations such as addition and subtraction. Furthermore, we define the operations running on MUL to take two clock cycles, and the ALU operations take one. This is definitely a simplified case from reality. However, it is a close enough approximation and does not change the generality of the results. Other choices can easily be implemented within our framework.

Since there is no widely distributed and recognized FDS implementation, we implemented our own. The implementation is based on [10] and has all the applicable refinements proposed in this paper, including multicycle operation support, resource preference control, and look ahead using the second order of displacement in force computation. Actually, based on our experience, the look-ahead function for FDS is very critical. Without invoking this mechanism, the basic FDS provides poor scheduling results even for small-sized examples. In Table II, we show the effect of look ahead for the HAL benchmark originally presented in [10], which has only 11 operations and

TABLE II
EFFECT OF LOOK-AHEAD MECHANISM IN FDS (RESULT SHOWN IN MUL/ALU NUMBER PAIR. DEADLINE IS IN CYCLES)

| deadline | w/t look-ahead | w/ look-ahead |
|---|---|---|
| 9 | (2 1) | (2 1) |
| 10 | (2 1) | (2 1) |
| 11 | (2 1) | (2 1) |
| 12 | **(3 1)** | **(2 1)** |
| 13 | **(3 1)** | **(1 1)** |
| 14 | **(3 1)** | **(1 1)** |

eight data dependencies. Because of this, in our experiments, the look-ahead function is always used to allow FDS to provide better results.

With the assigned resource/operation mapping, ASAP is first performed to find the critical path delay $L_c$. We then set our predefined deadline range to be $[L_c, 2L_c]$, i.e., from the critical path delay to two times of this delay. This results in 263 testing cases in total. For each delay, we run FDS first to obtain its scheduling result. Following this, the proposed MMAS algorithm is executed five times to obtain enough data for performance evaluation. We report the FDS result quality, the average and best result quality for the proposed algorithm, and the standard deviation for these results. The execution time information for both algorithms is also reported.

We have implemented our MMAS formulation in C for the TCS problem, with the refinements discussed in Section IV. The evaporation rate $\rho$ is configured to be 0.98. The scaling parameters for global and local heuristics are set to be $\alpha = \beta = 1$ and delivery rate $Q = 1$. These parameters are not changed over the tests. We also experimented with different ant numbers $m$ and the allowed iteration count $N$. For example, set $m$ to be proportional to the average branching factor of the DFG under study and $N$ to be proportional to the total operation number. However, it was found that there seems to exist a fixed value pair for $m$ and $N$ that works well across the wide range of testing samples in our benchmark. In our final settings, we set $m$ to be 10 and $N$ to be 150 for all the TCS experiments.

Due to the large amount of data, we will not be able to report testing results for all the 263 cases in detail. Table III compares the testing results for "idctcol" and invert_matrix_general, two of the biggest samples. In this table, we provide a side-by-side comparison between FDS and our proposed method. The scheduling results are reported as MUL/ALU number pair required by the obtained scheduling. For the MMAS method, we report both the average performance and the best performance in the five runs for each testing case together with the saving percentage. The saving is measured by the reduction of computing resources. In order to keep the evaluation general and objective, we use the total count of resources as the quality metrics without considering their individual cost factors.

Besides the absolute quality of the results, one difference between FDS and the proposed method is that our method is relatively more stable. In our experiments, it is observed that the FDS approach can provide the worse quality results as the deadline is relaxed. Using the "idctcol" in Table III as an example, FDS provides drastically worse results for deadlines ranging from 25 to 30, although it is able to reach decent scheduling qualities for deadline from 19 to 24. The same problem occurs for deadlines between 36 and 38. One possible reason is that as the deadline is extended, the time frame of each operation is also extended, which makes the force computation more likely to clash with similar values. Due to the lack of backtracking and good look-ahead capability, an early mistake would lead to inferior results. On the other hand, our proposed algorithm robustly generates monotonically nonincreasing results with fewer resource requirements as the deadline increases.

Table IV summarizes the testing results for all of the benchmarks. We present the average and the best results for each testing benchmark, its tested deadline range, and the average standard deviations. The table is arranged in increasing order of the complexity of the DFGs. The average result quality generated by our algorithm is better than or equal to the FDS results in 258 out of 263 cases. Among them, for 192 testing cases (or 73% of the cases), our MMAS method outperforms the FDS method. There are only five cases where our approach has worse average quality results. They all happened on the invert_matrix_general benchmark and are listed in Table III, indicated by lines with italic bold fonts. On average, as shown in Table IV, we can expect a 16.4% performance improvement over FDS. If only considering the best results among the five runs for each testing case, we achieve a 19.5% resource reduction averaged over all tested samples. The most outstanding results provided by our proposed method achieve a 75% resource reduction compared with FDS. These results are obtained on a few deadlines for the jpeg_idct_ifast benchmark.

From Table IV, it is easy to see that for all the examples, MMAS-based OS achieves better or much better results. Our approach seems to have much stronger capability in robustly finding better results for different testing cases. Furthermore, it scales very well over different DFG sizes and complexities. Another aspect of scalability is the predefined deadline. Based on the results presented in Tables III and IV, the proposed algorithm also demonstrates better scalability over this parameter.

All of the experimental results are obtained on a Linux box with a 2-GHz CPU. Fig. 4 shows the execution time comparison between the presented algorithm and the FDS. Curves A and B show the run time for FDS and the proposed method, respectively, where we use the average runtime for our MMAS solutions over five runs. As discussed before, since we use a fixed ant number $m$ and iteration limit $N$ in our experiments to make the algorithm simpler, there exists a big gap between the execution times for the smaller-sized cases. For example, for the HAL example, which only has 11 operations, the execution time of FDS is 0.014 s while our method takes 0.66 s. This translates into a ratio of 47. However, as the size of the problem gets bigger, this ratio drops quickly. For the biggest cases invert_matrix_general, FDS takes 270.6 s while our method spends about 411.7 s, which makes the ratio 1.5. To summarize, for smaller cases, our algorithm does have relatively larger execution times but the absolute run time is still very short. For the HAL example, it only takes a fraction of a second. For bigger cases, the proposed method has a runtime at the same scale as FDS. This makes our algorithm practical.

In Fig. 4, we do see some spikes in the ratio curve. We contribute this to two main reasons. First, the recorded execution time is based on system time, and it is relatively more unreliable

TABLE III
PARTIAL DETAILED RESULTS FOR TCS (SIZE IS GIVEN AS DFG NODE/EDGE NUMBER PAIR. VIRTUAL NODES AND EDGES ARE NOT COUNTED. AVERAGE AND STANDARD DEVIATION $\sigma$ ARE COMPUTED OVER FIVE RUNS. SAVING IS COMPUTED BASED ON FDS RESULTS. NO WEIGHT APPLIED)

| Name (size) | Deadline | FDS | Average | Savings | Best | Savings | $\sigma$ |
|---|---|---|---|---|---|---|---|
| idctcol (114 164) | 19 | (6 8) | (5.0 6.0) | 21.43% | (5 6) | 21.43% | 0.000 |
| | 20 | (5 7) | (4.4 6.0) | 13.33% | (4 6) | 16.67% | 0.219 |
| | 21 | (4 7) | (4.2 5.8) | 9.09% | (4 6) | 9.09% | 0.000 |
| | 22 | (4 7) | (4.2 5.4) | 12.73% | (4 5) | 18.18% | 0.219 |
| | 23 | (4 7) | (4.0 5.4) | 14.55% | (4 5) | 18.18% | 0.219 |
| | 24 | (4 7) | (3.6 5.2) | 20.00% | (3 5) | 27.27% | 0.335 |
| | 25 | **(8 8)** | (3.8 5.0) | 45.00% | (3 5) | 50.00% | 0.179 |
| | 26 | **(8 8)** | (3.4 5.0) | 47.50% | (3 5) | 50.00% | 0.219 |
| | 27 | **(8 8)** | (3.0 5.0) | 50.00% | (3 5) | 50.00% | 0.00 |
| | 28 | **(8 8)** | (3.0 4.6) | 52.50% | (3 4) | 56.25% | 0.219 |
| | 29 | **(8 8)** | (3.0 4.4) | 53.75% | (3 4) | 56.25% | 0.219 |
| | 30 | **(8 8)** | (3.0 4.6) | 52.50% | (3 4) | 56.25% | 0.219 |
| | 31 | (4 6) | (3.0 4.6) | 24.00% | (3 4) | 30.00% | 0.219 |
| | 32 | (4 5) | (3.0 4.0) | 22.22% | (3 4) | 22.22% | 0.000 |
| | 33 | (4 5) | (2.8 4.0) | 24.44% | (2 4) | 33.33% | 0.179 |
| | 34 | (4 5) | (3.0 4.0) | 22.22% | (3 4) | 22.22% | 0.000 |
| | 35 | (4 5) | (3.0 4.0) | 22.22% | (3 4) | 22.22% | 0.000 |
| | 36 | **(4 6)** | (3.0 3.8) | 32.00% | (3 3) | 40.00% | 0.179 |
| | 37 | **(4 6)** | (2.6 3.8) | 36.00% | (3 3) | 40.00% | 0.219 |
| | 38 | **(4 6)** | (2.8 3.4) | 38.00% | (3 3) | 40.00% | 0.179 |
| invert_matrix_general (333 354) | 15 | (24 23) | (26.0 22.0) | ***-2.13%*** | (25 22) | 0.00% | 0.283 |
| | 16 | (22 19) | (23.8 19.0) | ***-4.39%*** | (23 19) | ***-2.44%*** | 0.179 |
| | 17 | (19 17) | (21.8 17.4) | ***-8.89%*** | (21 17) | ***-5.56%*** | 0.335 |
| | 18 | (18 16) | (20.4 16.2) | ***-7.65%*** | (20 16) | ***-5.88%*** | 0.219 |
| | 19 | (17 16) | (19.2 16.0) | ***-6.67%*** | (19 15) | ***-3.03%*** | 0.335 |
| | 20 | (17 16) | (18.2 13.4) | 4.24% | (18 13) | 6.06% | 0.358 |
| | 21 | (16 16) | (17.2 12.8) | 6.25% | (17 13) | 6.25% | 0.000 |
| | 22 | (16 16) | (16.4 12.2) | 10.63% | (16 12) | 12.50% | 0.358 |
| | 23 | (16 16) | (16.0 11.8) | 13.12% | (16 11) | 15.62% | 0.179 |
| | 24 | (16 16) | (15.4 11.2) | 16.87% | (15 11) | 18.75% | 0.219 |
| | 25 | (16 16) | (14.4 10.8) | 21.25% | (14 11) | 21.88% | 0.179 |
| | 26 | (16 16) | (14.2 10.2) | 23.75% | (13 10) | 28.12% | 0.358 |
| | 27 | (16 16) | (13.8 10.0) | 25.62% | (13 10) | 28.12% | 0.179 |
| | 28 | (16 16) | (13.4 10.2) | 26.25% | (13 10) | 28.12% | 0.219 |
| | 29 | (16 16) | (13.0 9.4) | 30.00% | (13 9) | 31.25% | 0.219 |
| | 30 | (16 16) | (12.6 9.6) | 30.63% | (13 9) | 31.25% | 0.179 |

TABLE IV
RESULT SUMMARY FOR TCS DATA IN PARENTHESIS SHOWS THE RESULTS OBTAINED USING SA. DEADLINE SHOWS THE TESTED RANGE. AVERAGE $\sigma$ IS COMPUTED OVER THE TESTED RANGE. SAVING IS COMPUTED BASED ON FDS RESULTS. NO WEIGHT APPLIED

| Name | Size | Deadline | Avg. Savings (SA) | Best Savings (SA) | Avg. $\sigma$ (SA) |
|---|---|---|---|---|---|
| HAL | 11/8 | (6 - 12) | 7.1% (7.1%) | 7.1% (7.1%) | 0.000 (0.000) |
| horner_bezier_surf | 18/16 | (11 - 22) | 9.9% (-4.6%) | 13.2% (2.1%) | 0.015 (0.051) |
| ARF | 28/30 | (11 - 22) | 12.4% (-1.2%) | 16.9% (3.1%) | 0.093 (0.099) |
| motion_vectors | 32/29 | (7 - 14) | 13.1% (-3.4%) | 16.0% (2.8%) | 0.072 (0.177) |
| EWF | 34/47 | (17 - 34) | 11.5% (-4.4%) | 18.1% (4.7%) | 0.081 (0.136) |
| FIR2 | 40/39 | (12 - 24) | 16.8% (-15.7%) | 22.8% (-1.9%) | 0.106 (0.299) |
| FIR1 | 44/43 | (12 - 24) | 15.2% (-7.7%) | 18.0% (-3.3%) | 0.047 (0.116) |
| h2v2_smooth_downsample | 51/52 | (17 - 34) | 19.3% (7.6%) | 21.3% (11.0%) | 0.042 (0.088) |
| feedback_points | 53/50 | (11 - 22) | 5.9% (-12.8%) | 9.2% (-6.4%) | 0.103 (0.196) |
| collapse_pyr | 56/73 | (8 - 16) | 18.3% (4.6%) | 18.9% (9.6%) | 0.044 (0.195) |
| COSINE1 | 66/76 | (10 - 20) | 21.5% (7.4%) | 25.9% (14.1%) | 0.150 (0.349) |
| COSINE2 | 82/91 | (10 - 20) | 5.6% (-14.8%) | 12.0% (-7.3%) | 0.232 (0.342) |
| write_bmp_header | 106/88 | (8 - 16) | 0.9% (-5.3%) | 1.0% (-3.4%) | 0.064 (0.093) |
| interpolate_aux | 108/104 | (10 - 20) | 0.2% (-36.5%) | 2.0% (-27.9%) | 0.109 (0.407) |
| matmul | 109/116 | (11 - 22) | 3.7% (-30.8%) | 5.1% (-21.4%) | 0.088 (0.363) |
| idctcol | 114/164 | (19 - 38) | 30.7% (12.6%) | 34.0% (17.5%) | 0.151 (0.231) |
| jpeg_idct_ifast | 122/162 | (17 - 34) | 50.3% (36.9%) | 52.1% (41.8%) | 0.147 (0.336) |
| jpeg_fdct_islow | 134/169 | (16 - 32) | 31.4% (7.5%) | 34.2% (13.0%) | 0.171 (0.335) |
| smooth_color_z_triangle | 197/196 | (15 - 30) | 7.3% (-18.7%) | 9.2% (-12.0%) | 0.136 (0.472) |
| invert_matrix_general | 333/354 | (15 - 30) | 11.2% (-29.4%) | 13.2% (-22.9%) | 0.237 (0.743) |
| Total Avg. | | | 16.4% (-5.1%) | 19.5% (1.0%) | 0.104 (0.251) |

when the execution time is small. Second, but perhaps more important, the timing performance of both algorithms is not only determined by the DFG node count but also dependent on the predefined dependencies in the DFGs and the deadline $D$. This will introduce variance when the curves are drawn against the node count.

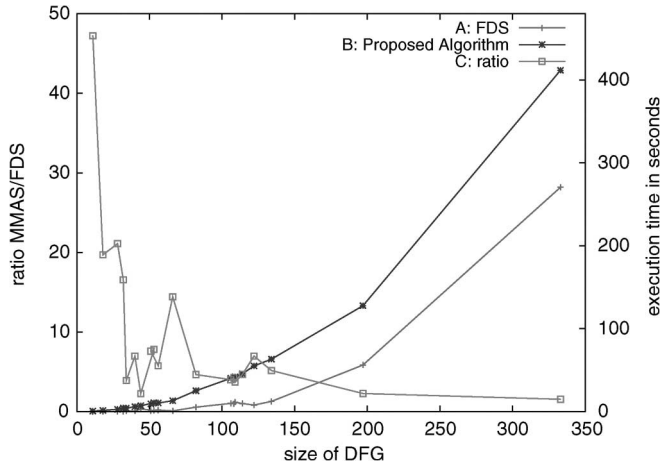


Fig. 4. Execution time for TCS. (Ratio is MMAS time/FDS time.)

### *B. RCS*

We have implemented the proposed MMAS-based RCS algorithm and compared its performance with the popularly used list-scheduling and FDS algorithms.

For each of the benchmark samples, we run the proposed algorithm with different choices of local heuristics. For each choice, we also perform five runs to obtain enough statistics for evaluating the stability of the algorithm. Again, we fixed the number of ants per iteration to ten, and in each run we allow 100 iterations. Other parameters are also the same as those used in the TCS problem. The best schedule latency is reported at the end of each run, and then the average value is reported as the performance for the corresponding setting. Two different experiments are conducted for RCS, namely: 1) the homogenous case and 2) the heterogeneous case.

For the homogenous case, resource allocation is performed before the OS. Each operation is mapped to a unique resource type. In other words, there is no ambiguity on which resource the operation shall be handled during the scheduling step. In this experiment, similar to the TCS case, two types of resources (MUL/ALU) are allowed. The number of each resource type is predefined after making sure they do not make the experiment trivial (for example, if we are too generous, then the problem simplifies to an ASAP problem).

Table V shows the testing results for the homogenous case. The best results for each case are shown in bold. Compared with a variety of list-scheduling approaches and the FDS method, the proposed algorithm generates better results consistently over all testing cases, which is demonstrated by the number of times that it provides the best results for the tested cases. This is especially true for the case when OD is used as the local heuristic, where we find the best results in 14 cases among 20 tested benchmarks. For other traditional methods, FDS generates the most hits (ten times) for best results, which is still less than the worst case of MMAS (11 times). For some of the testing samples, our method provides significant improvement on the schedule latency. The biggest saving achieved is 22%. This is obtained for the COSINE2 benchmark when OM is used as the local heuristic for our algorithm and also as the heuristic for constructing the priority list for the traditional list scheduler. For cases that our algorithm fails to provide the best solution, the quality of its results is also much closer to the best than other methods.

Besides the absolute schedule latency, another important aspect of the quality of a scheduling algorithm is its stability over different input applications. As indicated in Section II, the performance of the traditional list scheduler heavily depends on the input application. This is echoed by the data in Table V. In the meantime, it is easy to observe that the proposed algorithm is much less sensitive to the choice of different local heuristics and input applications. This is evidenced by the fact that the standard deviation of the results achieved by the new algorithm is much smaller than that of the traditional list scheduler. Based on the data shown in Table V, the average standard deviation for list scheduling over all the benchmarks and different heuristic choices is 1.2, while for the MMAS algorithm it is only 0.19. In other words, we can expect to achieve high-quality scheduling results much more stably on different application DFGs regardless of the choice of local heuristic. This is a great attribute desired in practice.

One possible explanation for the above advantage is the different way how the scheduling heuristics are used by the list scheduler and the proposed algorithm. In list scheduling, the heuristics are used in a greedy manner to determine the order of the operations. Furthermore, the schedule of the operations is done all at once. Differently, in the proposed algorithm, local heuristics are used stochastically and combined with the pheromone values to determine the operations' order. This makes the solution exploration more balanced. Another fundamental difference is that the proposed algorithm is an iterative process. In this process, the pheromone value acts as an indirect feedback and tries to reflect the quality of a potential component based on the evaluations of historical solutions that contain this component. It introduces a way to integrate global assessments into the scheduling process, which is missing in the traditional list or FDS.

In the second experiment, heterogeneous computing units are allowed, i.e., one type of operation can be performed by different types of resources. For example, multiplication can be performed by either a faster multiplier or a regular one. Furthermore, multiple same-type units are also allowed. For example, we may have three faster multipliers and two regular ones.

We conduct the heterogeneous experiments with the same configuration as for the homogenous case. Moreover, to better assess the quality of our algorithm, the same heterogeneous RCS tasks are also formulated as ILP problems and then optimally solved using CPLEX. Since the ILP solution is time consuming to obtain, our heterogeneous tests are only done for the classic samples.

Table VI summarizes our heterogeneous experimental results. Here, an extended HAL benchmark is used, which includes extra memory access operations. Compared with a variety of list-scheduling approaches and the FDS method, the proposed algorithm generates better results consistently over all testing cases. The biggest saving achieved is 23%. This is obtained for the FIR2 benchmark when the LWOD is used as the local heuristic. Similar to the homogenous case, our

TABLE V
RESULT SUMMARY FOR HOMOGENOUS RCS (HEURISTIC LABELS: OM = OPERATION MOBILITY, OD = OPERATION DEPTH, LWOD = LATENCY WEIGHTED OPERATION DEPTH, SN = SUCCESSOR NUMBER)

| Name | Size | Resources | FDS | List Scheduling | | | | MMAS(average over 5 runs) | | | | SA ( avg. 10 runs) |
|---|---|---|---|---|---|---|---|---|---|---|---|---|
| | | | | OM | OD | LWOD | SN | OM | OD | LWOD | SN | |
| HAL | (8/11) | (2 1) | **8** | 10 | **8** | **8** | **8** | **8.0** | **8.0** | **8.0** | **8.0** | **8.0** |
| horner_bezier_surf | (16/18) | (2 1) | **12** | 16 | **12** | 13 | 13 | **12.0** | **12.0** | **12.0** | **12.0** | 12.4 |
| ARF | (30/28) | (3 1) | 18 | 19 | **16** | 18 | 18 | **16.0** | **16.0** | **16.0** | **16.0** | 17.2 |
| motion_vectors | (29/32) | (3 4) | **12** | 15 | **12** | **12** | 14 | **12.0** | **12.0** | **12.0** | **12.0** | 13.3 |
| EWF | (47/34) | (1 2) | **21** | 22 | **21** | **21** | 22 | **21.0** | **21.0** | **21.0** | **21.0** | 21.3 |
| FIR2 | (39/40) | (2 3) | 17 | 19 | 18 | 17 | 15 | 17.0 | **16.8** | 17.0 | 17.0 | 18.5 |
| FIR1 | (43/44) | (2 3) | **16** | 22 | 22 | 21 | **16** | **16.0** | **16.0** | **16.0** | **16.0** | 21.1 |
| h2v2_smooth_downsample | (52/51) | (1 3) | 23 | 28 | 23 | 23 | **22** | 22.4 | 22.8 | 22.8 | 22.8 | 23.6 |
| feedback_points | (50/53) | (3 3) | 16 | 20 | **14** | 19 | **14** | 14.4 | 14.2 | 14.6 | 14.6 | 16.6 |
| collapse_pyr | (73/56) | (3 5) | **11** | 12 | **11** | **11** | **11** | **11.0** | **11.0** | **11.0** | **11.0** | 11.3 |
| COSINE1 | (76/66) | (4 5) | 16 | 18 | 16 | 17 | 16 | **14.0** | **14.0** | **14.0** | **14.0** | 15.2 |
| COSINE2 | (91/82) | (5 8) | 14 | 18 | 14 | 17 | 13 | **12.4** | **12.4** | 12.6 | 12.8 | 14.9 |
| write_bmp_header | (88/106) | (1 9) | **12** | 17 | **12** | **12** | **12** | 12.8 | 12.6 | 12.8 | 12.4 | 13.4 |
| interpolate_aux | (104/108) | (9 8) | 13 | 16 | 12 | 16 | 16 | **11.0** | 11.8 | **11.0** | 11.8 | 15.6 |
| matmul | (116/109) | (9 8) | 15 | 14 | **13** | 14 | 14 | 13.6 | 13.8 | 13.8 | 13.8 | 14.7 |
| idctcol | (164/114) | (5 6) | 21 | 26 | 21 | 21 | 21 | 20.6 | **19.8** | 20.2 | 20.0 | 24.3 |
| jpeg_idct_ifast | (162/122) | (10 9) | **19** | 21 | 20 | **19** | **19** | **19.0** | **19.0** | **19.0** | **19.0** | 20.8 |
| jpeg_fdct_islow | (169/134) | (5 7) | **21** | 28 | 22 | 22 | **21** | 22.0 | 22.0 | 21.8 | 21.8 | 23.8 |
| smooth_color_z_triangle | (196/197) | (8 9) | **24** | 25 | 25 | 23 | **24** | **24.0** | **24.0** | **24.0** | **24.0** | 25.5 |
| invert_matrix_general | (354/333) | (15 11) | 26 | 28 | 28 | 25 | 25 | **24.0** | **24.2** | **24.2** | **24.2** | 27.1 |

TABLE VI
RESULT SUMMARY FOR HETEROGENEOUS RCS SCHEDULE LATENCY IS IN CYCLES; RUNTIME IS IN SECONDS; † INDICATES CPLEX FAILED TO PROVIDE FINAL RESULT BEFORE RUNNING OUT OF MEMORY. (RESOURCE LABELS: A = ALU, FM = FASTER MULTIPLIER, M = MULTIPLIER, I = INPUT, O = OUTPUT) (HEURISTIC LABELS: OM = OPERATION MOBILITY, OD = OPERATION DEPTH, LWOD = LATENCY WEIGHTED OPERATION DEPTH, SN = SUCCESSOR NUMBER)

| Benchmark (nodes/edges) | Resources | CPLEX (latency/runtime) | Force Directed | List Scheduling | | | | MMAS(average over 5 runs) | | | |
|---|---|---|---|---|---|---|---|---|---|---|---|
| | | | | OM | OD | LWOD | SN | OM | OD | LWOD | SN |
| HAL(21/25) | 1a, 1fm, 1m, 3i, 3o | 8 / 32 | **8** | **8** | **8** | 9 | **8** | **8** | **8** | **8** | **8** |
| ARF(28/30) | 2a, 1fm, 2m | 11 / 22 | **11** | **11** | 13 | 13 | 13 | **11** | **11** | **11** | **11** |
| EWF(34/47) | 1a, 1fm, 1m | 27 / 24000 | 28 | 28 | 31 | 31 | 28 | 27.2 | 27.2 | **27** | 27.2 |
| FIR1(40/39) | 2a, 2m, 3i, 3o | 13 / 232 | 19 | 19 | 19 | 19 | 18 | 17.2 | 17.2 | **17** | 17.8 |
| FIR2(44/43) | 1a, 1fm, 1m, 3i, 3o | 14 / 11560 | 19 | 19 | 21 | 21 | 21 | **16.2** | 16.4 | **16.2** | 17 |
| COSINE1(66/76) | 2a,2m, 1fm, 3i, 3o | † | 18 | 19 | 20 | 18 | 18 | **17.4** | 18.2 | 17.6 | 17.6 |
| COSINE2(82/91) | 2a,2m, 1fm, 3i, 3o | † | 23 | 23 | 23 | 23 | 23 | **21.2** | **21.2** | **21.2** | **21.2** |

algorithm outperforms other methods with regards to consistently generating high-quality results. In Table VI, the average standard deviation for the list scheduler over all the benchmarks and different heuristic choices is 0.8128, while that for the MMAS algorithm is only 0.1673.

Although the results of the force-directed scheduler generally outperform the list scheduler, our algorithm achieves even better results. On average, comparing with the force-directed approach, our algorithm provides a 6.2% performance enhancement for the testing cases, while the performance improvement for individual test sample can be as much as 14.7%.

Finally, compared with the optimal scheduling results computed by using the ILP model, the results generated by the proposed algorithm are much closer to the optimal than those provided by the list-scheduling heuristics and the force-directed approach. For all the benchmarks with known optima, our algorithm improves the average schedule latency by 44% compared with the list-scheduling heuristics. For larger-sized DFGs such as COSINE1 and COSINE2, CPLEX fails to generate optimal results after more than 10 h of execution on a Scalable Performance ARChitecture (SPARC) workstation with a 440-MHz CPU and 384-MB memory. In fact, CPLEX crashes for these two cases because of running out of memory. For COSINE1, CPLEX does provide an intermediate suboptimal solution of 18 cycles before it crashes. This result is worse than the best result found by our proposed algorithm.

The experimental results of our algorithm as well as those for list scheduling and the FDS are obtained on a Linux box with a 2-GHz CPU. For all the benchmarks, the runtime of the proposed algorithm ranges from 0.1 to 1.76 s. List scheduling is always the fastest due to its one-pass nature. It typically finishes within a small fraction of a second. The force-directed scheduler runs much slower than the list scheduler because its complexity is cubic in the number of operations. For small testing cases, it is typically faster than our algorithm as we set a fixed iteration number for the ants to explore the search space. However, as the problem size grows, the force-directed scheduler has longer runtime than our algorithm. In fact, for COSINE1 and COSINE2, the force-directed approach takes 12.7% and 21.2% more execution time, respectively.

The evolutionary effect on the global heuristics $\tau_{ij}$ is illustrated in Fig. 6. It plots the pheromone values for the ARF testing sample after 100 iterations of the proposed algorithm. The $x$-axis is the index of operation node in the DFG (shown

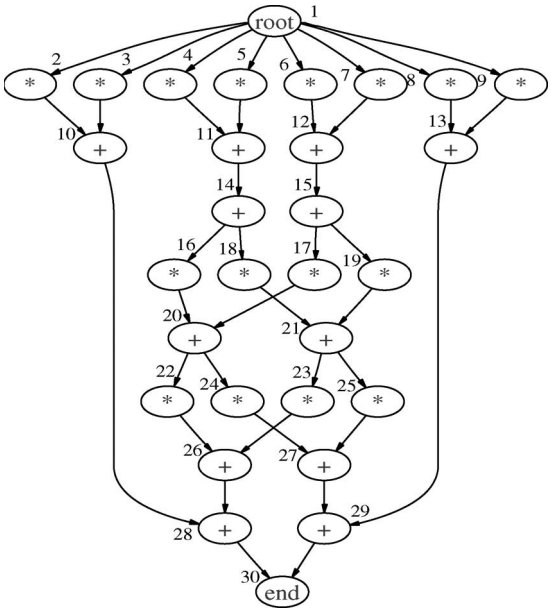


Fig. 5. DFG. (The number by the node is the index assigned for the operation.)

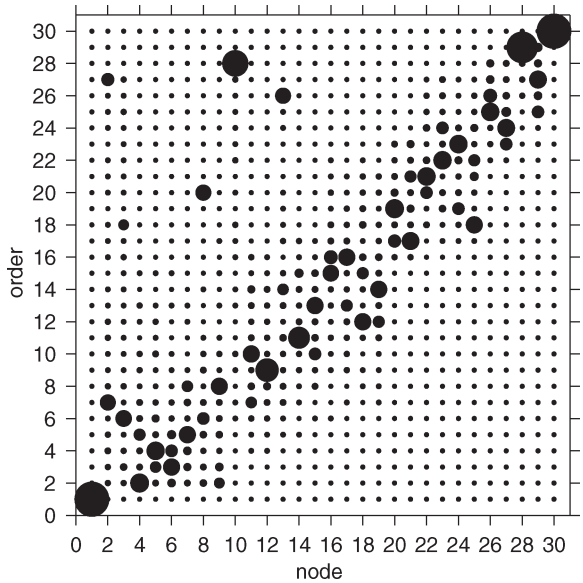


Fig. 6. Pheromone heuristic distribution for ARF.

in Fig. 5), and the $y$-axis is the order index in the priority list passed to the list scheduler. There exist totally 30 nodes with node 1 and node 30 as the dummy source and sink of the DFG, respectively. Each dot in the diagram indicates the strength of the resultant pheromone trails for assigning a corresponding order to a certain operation—the bigger the size of the dot, the stronger the value of the pheromone.

It is clearly seen in Fig. 6 that there are a few strong pheromone trails while the remaining pheromone trails are very weak. This might be explained by the strong symmetric structure of the ARF DFG and the special implementation in our algorithm of considering operation list only with topologically sorted order. It is also interesting to notice that although a good amount of operations have a limited few alternative "good" positions (such as operation 6 and 26), for some of the operations, the pheromone heuristics are strong enough to lock their positions. For example, according to its pheromone distribution, operation 10 shall be placed as the 28th item in the list, and there is no other competitive position for its placement. After careful evaluation, this ordering preference cannot be trivially obtained by constructing priority lists with any of the popularly used heuristics. This shows that the proposed algorithm has the possibility to discover better orderings that may be hard to achieve intuitively.

### C. Comparison With SA

In order to further investigate the quality of the proposed algorithms, we compared them with the SA approach. For RCS, we implemented the algorithm presented in [21]. The basic idea is very similar to what we proposed in our MMAS approach in which a metaheuristic method (SA) is used to guide the searching process while a traditional list scheduler is used to evaluate the result quality. The scheduling result with the best resource usage is reported when the algorithm terminates.

However, it is more difficult for the TCS problem since we have not found any SA-based approach in previously published works. Therefore, we formulated one ourselves. Consequently, we will give more emphasis on our SA-based formulation for the TCS problem in the rest of this section.

A pseudo-implementation of the SA-based TCS algorithm is given in Algorithm 3.

**Algorithm 3:** SA for TCS
**procedure** SA-TCS($G$, $R$)
**input**: DFG $G(V, E)$, resource set $R$, and a map of operation to one resource in $R$
**output**: operation schedule
1: perform ASAP and ALAP on the DFG to obtain mobility ranges.
2: randomly initialize a valid seed scheduling $S_{current}$
3: set starting and ending temperature $T_s$ and $T_e$.
4: set local search weight to $\theta$.
5: set $N$ to be the number of operations.
6: set $t$ to $T_s$
7: set $S_{best}$ to be $S_{current}$
8: **while** $t > T_e$ **do**
9: for $I = 0; i < \theta N;$ i + + **do**
10: randomly generate a neighbor solution $S_n$
11: **if** $S_n$ is invalid **then**
12: continue
13: **else**
14: compute the resource cost of $S_n$
15: randomly accept $S_n$ to be $S_{current}$
16: update $S_{best}$ if needed
17: **end if**
18: **end for**
19 update $t$ based on cooling scheme
20: **end while**
21: return $S_{best}$ and the resource cost

The major challenge here is the construction of a "neighbor" selection in the SA process. With knowledge of each

operation's mobility range, it is trivial to see that the search space for the TCS problem is covered by all the possible combinations of operation/time step pairs, where each operation can be scheduled into any time step in its mobility range. In our formulation, given a scheduling $S$ where operation $op_i$ is scheduled at $t_i$, we experimented with two different methods for generating a neighbor solution.

1) Physical neighbor: A neighbor of $S$ is generated by selecting an operation $op_i$ and rescheduling it to a physical neighbor of its current scheduled time step $t_i$, namely either $t_i + 1$ or $t_i - 1$ with even possibility. In case $t_i$ is on the boundary of its mobility range, we treat the mobility range as a circular buffer.
2) Random neighbor: A neighbor of $S$ is generated by selecting an operation and rescheduling it to any of the positions in its mobility range excluding its currently scheduled position.

However, both of the above approaches suffer from the problem that many of these "neighbors" will be invalid because they may violate the data dependency posed by the DFG. For example, say, in $S$, a single cycle operation $op_1$ is scheduled at time step 3, and another single cycle operation $op_2$ that is data dependent on $op_1$ is scheduled at time step 4. Changing the schedule of $op_2$ to step 3 will create an invalid scheduling result. To deal with this problem in our implementation, for each generated scheduling, we quickly check whether it is valid by verifying the operation's new schedule against those of its predecessor and successor operations defined in the DFG. Only valid schedules will be considered.

Furthermore, in order to give roughly equal chance for each operation to be selected in the above process, we try to generate multiple neighbors before any temperature update is taken. This can be considered as a local search effort, which is widely implemented in different variants of the SA algorithm. We control this local search effort with a weight parameter $\theta$. That is, before any temperature update takes place, we attempt to generate $\theta N$ valid scheduling candidates, where $N$ is the number of operations in the DFG. In this paper, we set $\theta = 2$, which roughly gives each operation two chances to alter its currently scheduled position in each cooling step.

This local search mechanism is applied to both neighbor generation schemes discussed above. In our experiments, we found that there is no noticeable difference between the two neighbor generation approaches with respect to the quality of the final scheduling results except that the "random neighbor" method tends to take significantly more computing time. This is because it is more likely to come up with an invalid scheduling that is simply ignored in our algorithm. In our final realization, we always use the "physical neighbor" method.

Another issue related to the SA implementation is how to set the initial seed solution. In our experiments, we experimented with three different seed solutions: ASAP, ALAP, and a randomly generated valid scheduling. We found that the SA algorithm with a randomly generated seed constantly outperforms that using the ASAP or ALAP initialization. It is especially true when the "physical neighbor" approach is used. This is not surprising since the ASAP and ALAP solutions tend to cluster operations together, which is bad for minimizing resource usage. In our final realization, we always use the randomly generated schedule as the seed solution.

The framework of our SA implementation for both TCS and RCS is similar to the one reported in [44]. The acceptance of a more costly neighboring solution is determined by applying the Boltzmann probability criteria [45], which depends on the cost difference and the annealing temperature. In our experiments, the most commonly known and used geometric cooling schedule [44] is applied, and the temperature decrement factor is set to 0.9. When it reaches the predefined maximum iteration number or the stop temperature, the best solution found by SA is reported.

The experimental results for the TCS problem obtained using the above SA formulation are shown in Table IV, where the SA results are provided in parenthesis column-by-column with those achieved by using MMAS. Similar to the MMAS algorithm, we perform five runs for each benchmark sample and report the average savings, the best savings, and the standard deviation of the reported scheduling results. It can be seen from Table IV that the SA method provides much worse results compared with the proposed MMAS solutions. In fact, the MMAS approach provides better results on every testing case. Although the SA method does have significant gains on select cases over FDS, its average performance is actually worse than FDS by 5%, while our method provides a 16.4% average savings. This is also true if we consider the best savings achieved among multiple runs, where a modest 1% savings is observed in SA compared with a 19.5% reduction obtained by the MMAS method. Furthermore, the quality of the SA method seems to be very dependent on the input applications. This is evidenced by the large dynamic range of the scheduling quality and the larger standard deviation over the different runs. Finally, we also want to make it clear that to achieve this result, the SA approach takes substantially more computing time than the proposed MMAS method. A typical experiment over all 263 testing cases will run between 9 and 12 h, which is three to four times longer than the MMAS-based TCS algorithm.

As discussed above, our SA formulation for RCS is similar to that studied in [21]. It is relatively more straight forward since it will always provide valid scheduling using a list scheduler. To be fair, a randomly generated operation list is used as the seed solution for the SA algorithm. The neighbor solutions are constructed by swapping the positions of two neighboring operations in the current list. Since the algorithm always generates a valid scheduling, we can better control the runtime than in its TCS counterpart by adjusting the cooling scheme parameter. We carried experiments using execution limit ranging from one to ten times that of the MMAS approach. It was observed that the SA RCS algorithm provides poor performance when the time limit was too short. On the other hand, once we increase this time limit to over five times of the MMAS execution time, there was no significant improvement on the results as the execution time increased. In the rightmost column of Table V, we present the typical RCS results using SA achieved with ten times the MMAS execution time. The performance data are averaged over ten runs for each testing sample. It is easy to see that the MMAS-based algorithm consistently outperforms it while using much less computing time.

### D. Parameter Sensitivity

The proposed ACO-based algorithms belong to the category of stochastic search algorithms. This implies a certain sensitivity of the result to the choices of parameters that are at times difficult to determine. In order to better understand this issue and its relationship with the algorithms' performance, a study on their sensitivity to the parameter selection is in order. We have conducted extensive experiments in this paper on this topic and will report our major findings in this section.

*1) $\alpha$, $\beta$, and $Q$:* Variation on the global heuristic weight $\alpha$, the local heuristic weight $\beta$, and the pheromone delivery constant $Q$ does not have noticeable impact on the performance of our algorithms. The algorithms consistently provide robust results when $\alpha$ and $\beta$ are in the range of [1, 100] and $Q$ is between [1, 5000] with small step size, while performance on benchmarks of smaller sizes tends to have more fluctuations than the bigger ones. Of course, a numerically precise limit should be a concern for the parameters $\alpha$ and $\beta$ in algorithm realization because they are used in power functions. Also, the scaling of local and global heuristics could be an issue with these parameters. In our study, we found that setting $\alpha = \beta = 1$ worked well in our implementation over a comprehensive set of testing benchmarks. Moreover, the benefit is that it essentially eliminates the power function calls in (1), which further reduces the computing time.

*2) $\rho$:* The pheromone evaporation factor $\rho$ takes a value in the range of [0, 1] and controls how much the existing pheromone trails will be reduced before any enhancement. The smaller is this number, the more reduction is applied [see (2)]. When this number is too small, historical information accumulated in the search process will be essentially lost, and the algorithms behave close to a random search. In our experiments, we found that a value between 0.95 and 1 seems to be a good choice. In our final setup, the parameter $\rho$ is set to 0.98.

*3) $p_{\text{best}}$:* This parameter, together with $\rho$, controls how the lower bound and upper bound of pheromone trails will be computed. Recall that when $p_{\text{best}} \to 0$, the difference between $\tau_{\min}(t)$ and $\tau_{\max}(t)$ gets smaller, which means the search is getting more random and more emphasis is given to search space exploration. In our experiments, we found that $p_{\text{best}}$ should be bigger than 0.5. Once it is above this threshold, both algorithms for RCS and TCS problems perform robustly. In our final setup, $p_{\text{best}}$ is set to 0.93.

*4) $m$ and $N$:* The ant count $m$ and the iteration number $N$ are closely related and have a direct impact on the algorithms execution time. Roughly, the product of $m$ and $N$ gives an estimation of how many scheduling instances the algorithms will cover. Theoretically, the bigger is this product, the better is the performance. Also, it is intuitive to see that these parameters should be positively correlated with the complexity of the test sample. In this paper, we prefer to use a fixed setting for these parameters in order to make the algorithm simpler. As reported above, with $m = 10$ and $N$ is set to be 150 and 100 for the TCS and RCS problem, respectively, our algorithms work well over a wide range of testing samples. In a further study, we varied $m$ between 1 and 10, and $N$ from 50 to 1000. We found that little performance improvement is seen after $N$ is bigger than 250 when $m$ is reasonably large ($\geqslant 4$). We contribute this to the fact that the pheromone trails converge after a large number of iterations. If $N$ is smaller than 100, we will often miss the optimal solution because of premature termination. This is especially true for the TCS problem. Similarly, when $m$ is bigger than 6, we see little improvement. The best tradeoff of $m$ seems to be between 4 and 6. It is interesting to notice that these numbers are very close to the average branching factor of the testing samples. These results imply that we may still have room to fine tune these two parameters to further improve the performance/cost tradeoff of the algorithms.

## VIII. Related Work

To the best of our knowledge, the only other reported work on using ACO to solve the OS problem is done by Kopuri and Mansouri [46]. Compared with this paper, their study is limited to the TCS problem.

To address the TCS problem, their algorithm has a different formulation and is more closely related to the classic FDS algorithm. They use a modified self-force computation, where predecessor and successor forces are dropped in the overall force consideration. This force is calculated by linear combination of normalized classic self-force and the pheromone trails. Since the resulting value can be both negative and positive, it is hard to act as an indicator for operation selection during the scheduling construction process. In their work, simple random selection is used.

Our algorithm uses a dynamically computed distribution graph for the corresponding resource $k$ for the local heuristic, and force calculation is not needed. We believe it provides the following benefits.

1) It is directly tied with the optimization target, i.e., minimizing the resource cost.
2) It is faster to compute.
3) The value range for the distributed graph is nonnegative, which enables more effective operation selection strategy than random selection as discussed in Section IV-C.

Moreover, as discussed in Section IV, our algorithm can be readily extended to handle different design scenarios such as multiple-cycle operations, mutually exclusive operations, operation chaining, and pipelining. It is unclear if their algorithm can be easily extended to do so, and only single-cycle operations were used in their study.

It is known that premature convergence is an important issue in ant-based approaches, and our experience shows that this is an important factor for the OS problem. In order to cope with this, the MAX–MIN formulation is used in our algorithms for both TCS and RCS. No such mechanism was used in [46].

Finally, the effectiveness and efficiency of our algorithms are tested over a comprehensive benchmark suite compiled from real-world applications. The performance with respect to solution quality, stability, scalability, and timing performance is more thoroughly studied and reported here. Only limited results on a small number of samples were reported in [46].

## IX. Conclusion

In this paper, we presented two novel heuristic searching methods for the RCS and TCS problems based on MMAS. Our algorithms employ a collection of agents that collaborate to explore the search space. We proposed a stochastic decision-making strategy in order to combine global and local heuristics to effectively conduct this exploration. As the algorithms proceed in finding better quality solutions, dynamically computed local heuristics are utilized to better guide the searching process.

A comprehensive set of benchmarks was constructed to include a wide range of applications. Experimental results over our test cases showed promising results. The proposed algorithms consistently provided higher quality results over the tested examples and achieved very good savings compared with traditional SA, list scheduling, and FDS approaches. Furthermore, the algorithm demonstrated robust stability over different applications and different selection of local heuristics, as evidenced by a much smaller deviation over the results.

## References


[1] Semiconductor Industry Association, *National Technology Roadmap for Semiconductors*, 2003.

[2] K. Kennedy and R. Allen, *Optimizing compilers for modern architectures: A dependence-based approach*. San Mateo, CA: Morgan Kaufmann, 2001.

[3] A. Aletà, J. M. Codina, J. Sánchez, and A. González, "Graph-partitioning based instruction scheduling for clustered processors," in *Proc. 34th Annu. ACM/IEEE Int. Symp. Microarchitecture*, 2001, pp. 150–159.

[4] G. D. Micheli, *Synthesis and Optimization of Digital Circuits*. New York: McGraw-Hill, 1994.

[5] J. E. Smith, "Dynamic instruction scheduling and the astronautics ZS -1," *Computer*, vol. 22, no. 7, pp. 21–35, Jul. 1989.

[6] T. Stützle and H. H. Hoos, "MAX–MIN ant system," *Future Gener. Comput. Syst.*, vol. 16, no. 9, pp. 889–914, Sep. 2000.

[7] H. Topcuouglu, S. Hariri, and M. You Wu, "Performance-effective and low-complexity task scheduling for heterogeneous computing," *IEEE Trans. Parallel Distrib. Syst.*, vol. 13, no. 3, pp. 260–274, Mar. 2002.

[8] D. Bernstein, M. Rodeh, and I. Gertner, "On the complexity of scheduling problems for parallel/pipelined machines," *IEEE Trans. Comput.*, vol. 38, no. 9, pp. 1308–1313, Sep. 1989.

[9] K. Wilken, J. Liu, and M. Heffernan, "Optimal instruction scheduling using integer programming," in *Proc. ACM SIGPLAN Conf. Program. Language Des. and Implementation*, 2000, pp. 121–133.

[10] P. G. Paulin and J. P. Knight, "Force-directed scheduling in automatic data path synthesis," in *Proc. 24th ACM/IEEE Conf. Des. Autom. Conf.*, 1987, pp. 195–202.

[11] P. G. Paulin and J. P. Knight, "Force-directed scheduling for the behavioral synthesis of ASIC's," *IEEE Trans. Comput.-Aided Design Integr. Circuits Syst.*, vol. 8, no. 6, pp. 661–679, Jun. 1989.

[12] W. F. J. Verhaegh, E. H. L. Aarts, J. H. M. Korst, and P. E. R. Lippens, "Improved force-directed scheduling," in *Proc. EURO-DAC*, 1991, pp. 430–435.

[13] W. F. J. Verhaegh, P. E. R. Lippens, E. H. L. Aarts, J. H. M. Korst, A. van der Werf, and J. L. van Meerbergen, "Efficiency improvements for force-directed scheduling," in *Proc. IEEE/ACM Int. Conf. Comput.-Aided Des.*, 1992, pp. 286–291.

[14] I.-C. Park and C.-M. Kyung, "Fast and near optimal scheduling in automatic data path synthesis," in *Proc. 28th ACM/IEEE DAC*, 1991, pp. 680–685.

[15] B. W. Kernighan and S. Lin, "An efficient heuristic procedure for partitioning graphs," *Bell Syst. Tech. J.*, vol. 49, no. 2, pp. 291–307, Feb. 1970.

[16] M. Heijligers and J. Jess, "High-level synthesis scheduling and allocation using genetic algorithms based on constructive topological scheduling techniques," in *Proc. Int. Conf. Evol. Comput.*, Perth, Australia, 1995, pp. 56–61.

[17] A. Sharma and R. Jain, "Insyn: Integrated scheduling for DSP applications," in *Proc. DAC*, 1993, pp. 349–354.

[18] T. L. Adam, K. M. Chandy, and J. R. Dickson, "A comparison of list schedules for parallel processing systems," *Commun. ACM*, vol. 17, no. 12, pp. 685–690, 1974.

[19] M. Grajcar, "Genetic list scheduling algorithm for scheduling and allocation on a loosely coupled heterogeneous multiprocessor system," in *Proc. 36th ACM/IEEE Conf. Des. Autom. Conf.*, 1999, pp. 280–285.

[20] S. J. Beaty, "Genetic algorithms versus tabu search for instruction scheduling," in *Proc. Int. Conf. Artif. Neural Nets and Genetic Algorithms*, 1993, pp. 496–501.

[21] P. H. Sweany and S. J. Beaty, "Instruction scheduling using simulated annealing," in *Proc. 3rd Int. Conf. Massively Parallel Comput. Syst.*, 1998.

[22] R. Kolisch and S. Hartmann, *Project Scheduling: Recent Models, Algorithms and Applications*. Norwell, MA: Kluwer, 1999, ch. Heuristic Algorithms for Solving the Resource-Constrained Project Scheduling problem: Classification and Computational Analysis.

[23] A. Auyeung, I. Gondra, and H. K. Dai, *Advances in Soft Computing: Intelligent Systems Design and Applications*. New York: Springer-Verlag, 2003, ch. Integrating random ordering into multi-heuristic list scheduling genetic algorithm.

[24] M. Dorigo, V. Maniezzo, and A. Colorni, "Ant system: Optimization by a colony of cooperating agents," *IEEE Trans. Syst., Man Cybern. B, Cybern.*, vol. 26, no. 1, pp. 29–41, Feb. 1996.

[25] J. L. Deneubourg and S. Goss, "Collective patterns and decision making," *Ethol., Ecol. Evol.*, vol. 1, no. 4, pp. 295–311, Dec. 1989.

[26] S. Fenet and C. Solmon, "Searching for maximum cliques with ant colony optimization," in *Proc. 3rd Eur. Workshop Evol. Comput. Combinatorial Optimization*, Apr. 2003, pp. 236–245.

[27] L. M. Gambardella, E. D. Taillard, M. Dorigo, "Ant colonies for the quadratic assignment," *J. Oper. Res. Soc.*, vol. 50, no. 2, pp. 167–176, 1996.

[28] D. Costa and A. Hertz, "Ants can colour graphs," *J. Oper. Res. Soc.*, vol. 48, no. 3, pp. 295–305, Mar. 1996.

[29] G. Leguizamon and Z. Michalewicz, "A new version of ant system for subset problems," in *Proc. Congr. Evol. Comput.*, 1999, pp. 1459–1464.

[30] R. Michel and M. Middendorf, *New Ideas in Optimization*. London, U.K.: McGraw-Hill, 1999, ch. An ACO algorithm for the shortest supersequence problem, pp. 51–61.

[31] S. Fidanova, "Evolutionary algorithm for multiple knapsack problem," in *Proc. PPSN-VII*, 2002, pp. 42–43.

[32] L. M. Gambardella, E. D. Taillard, and G. Agazzi, *New Ideas in Optimization*. London, U.K.: McGraw-Hill, 1999, ch. A multiple ant colony system for vehicle routing problems with time windows, pp. 51–61.

[33] R. S. Parpinelli, H. S. Lopes, and A. A. Freitas, "Data mining with an ant colony optimization algorithm," *IEEE Trans. Evol. Comput.*, vol. 6, no. 4, pp. 321–332, Aug. 2002.

[34] R. Schoonderwoerd, O. Holland, J. Bruten, and L. Rothkrantz, "Ant-based load balancing in telecommunications networks," *Adapt. Behav.*, vol. 5, no. 2, pp. 169–207, 1996.

[35] G. Wang, W. Gong, and R. Kastner, "A new approach for task level computational resource bi-partitioning," in *Proc. 15th Int. Conf. Parallel and Distrib. Comput. and Syst.*, Nov. 2003, vol. 1, no. 1, pp. 439–444.

[36] G. Wang, W. Gong, and R. Kastner, "System level partitioning for programmable platforms using the ant colony optimization," in *Proc. 13th IWLS*, Jun. 2004, pp. 238–245.

[37] G. Wang, W. Gong, and R. Kastner, "Application partitioning on programmable platforms using the ant colony optimization," *J. Embedded Comput.*, vol. 2, no. 1, pp. 119–136, 2006.

[38] W. J. Gutjahr, "ACO algorithms with guaranteed convergence to the optimal solution," *Inf. Process. Lett.*, vol. 82, no. 3, pp. 145–153, 2002.

[39] G. Pruesse and F. Ruskey, "Generating linear extensions fast," *SIAM J. Comput.*, vol. 23, no. 2, pp. 373–386, 1994.

[40] C. Lee, M. Potkonjak, and W. H. Mangione-Smith, "MediaBench: A tool for evaluating and synthesizing multimedia and communications systems," in *Proc. 30th Annu. ACM/IEEE Int. Symp. Microarchitecture*, 1997, p. 330.

[41] G. Aigner, A. Diwan, D. L. Heine, M. S. Lam, D. L. Moore, B. R. Murphy, and C. Sapuntzakis, *The Basic SUIF Programming Guide*. Stanford, CA: Comput. Syst. Lab., Stanford Univ., Aug. 2000.

[42] M. D. Smith and G. Holloway, *An Introduction to Machine SUIF and Its Portable Libraries for Analysis and Optimization*. Cambridge, MA: Division Eng. Appl. Sci., Harvard Univ., Jul. 2002.

[43] G. Wang, W. Gong, B. DeRenzi and R. Kastner, ExpressDFG benchmark suite. [Online]. Available: http://express.ece.ucsb.edu/benchmark/

[44] T. Wiangtong, P. Y. K. Cheung, and W. Luk, "Comparing three heuristic search methods for functional partitioning in hardware–software codesign," *Des. Autom. Embed. Syst.*, vol. 6, no. 4, pp. 425–429, Jul. 2002.

[45] E. Aarts and J. Korst, *Simulated Annealing and Boltzmann Machines: A Stochastic Approach to Combinatoria Optimization and Neural Computing*. New York: Wiley, 1989.

[46] S. Kopuri and N. Mansouri, "Enhancing scheduling solutions through ant colony optimization," in *Proc. ISCAS*, May 2004, pp. V-257–wV-260.

**Gang Wang** (M'98) received the B.S. degree in electrical engineering from Xi'an Jiaotong University, Xi'an, China, in 1992 and the M.S. degree in computer science from the Chinese Academy of Sciences, Beijing, China, in 1995. He is currently working toward the Ph.D. degree in the Department of Electrical and Computer Engineering, University of California, Santa Barbara.

From 1995 to 1997, he conducted research at Michigan State University, East Lansing, and Carnegie Mellon University, Pittsburgh, PA, focusing on speech and image understanding. Since 1997, he has held leading engineering positions in different companies, including Computer Motion Inc., Intuitive Surgical Inc., and Karl Storz Corp., focusing on the research and development of surgical robotics systems and intelligent operating rooms. He is currently with the Department of Electrical and Computer Engineering, University of California, Santa Barbara. His research areas include evolutionary computation, reconfigurable computing, nanocomputing, computer-aided design, and design automation.

**Wenrui Gong** (S'02) received the B.Engr. degree in computer science from Sichuan University, Sichuan, China, in 1999 and the M.Sc. degree in electrical and computer engineering from the University of California, Santa Barbara, in 2002. He is currently working toward the Ph.D. degree at the same university.

He joined the Catapult C Synthesis Group of Mentor Graphics Corporation, Wilsonville, OR, in October 2006. His research interests include architectural synthesis of electronic systems, compilation techniques, novel computing architectures, and optimization algorithms.

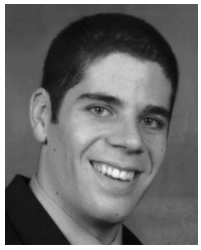

**Brian DeRenzi** (S'06) received the B.S. degree in computer engineering from the University of California, Santa Barbara, in 2006. He is currently working toward the M.S./Ph.D. degree in the Department of Computer Science and Engineering, University of Washington. His undergraduate research focused on high-level synthesis and compilation techniques for reconfigurable systems.

His current research interests focus on user-centered design and appropriate technology for the developing world.

**Ryan Kastner** (S'00–M'04) received the B.S. degrees in electrical engineering and computer engineering and the M.S. degree in engineering from Northwestern University, Evanston, IL, in 1999 and 2000, respectively, and the Ph.D. degree in computer science from the University of California, Los Angeles, in 2002.

He is an Associate Professor with the Department of Electrical and Computer Engineering, University of California, Santa Barbara. He has published over 70 technical articles and is the author of the book *Synthesis Techniques and Optimizations for Reconfigurable Systems* (Kluwer Academic Publishing, now Springer). His research interests lie in the realm of embedded system design, in particular, the use of reconfigurable computing devices for digital signal processing.

Dr. Kastner is a member of numerous conference technical committees including the International Conference on Computer Aided Design (ICCAD), the Design Automation Conference (DAC), the Design, Automation and Test in Europe, GLOBECOM, the International Conference on Computer Design (ICCD), the Great Lakes Symposium on VLSI (GLSVLSI), the International Conference on Engineering of Reconfigurable Systems and Algorithms (ERSA), and the International Symposium on Circuits and Systems (ISCAS). He serves on the editorial board for the *Journal of Embedded Computing*.